THE AMERICAN MINERALOGIST
JOURNAL OF THE MINERALOGICAL SOCIETY OF AMERICA

Vol. 29 JANUARY-FEBRUARY, 1944 Nos. 1 and 2

COMPOSITION OF SOME CHROMITES OF THE WESTERN HEMISPHERE

ROLLIN E. STEVENS, *U. S. Geological Survey, Washington, D. C.**

CONTENTS

Introduction 2
Composition and uses of chromite 3
Composition of chromites from the Western Hemisphere 4
  I. General plan of the analyses 4
  II. Complete analyses 5
  III. Partial analyses 16
  IV. Summary of analyses 23
Isomorphism in chromite 23
  I. Previous work, and purposes of study of isomorphism 23
  II. The spinel group 24
  III. Variation in the size of the unit cell of chromites of different compositions 25
  IV. Calculation of the ionic content of chromite unit cells from the analyses 27
  V. The spinel triangular prism of composition 29
  VI. Composition types in chromium-bearing spinel minerals 31
  VII. Expression of analyses in terms of end-members 33
Acknowledgments 34

ABSTRACT

The results are given of 52 complete and 144 partial analyses of purified chromite from deposits in the Western Hemisphere. The analyses show, in general, the grade of chromite at the various localities studied and the complete analyses are used to interpret isomorphism in chromites.

The major constituents of chromite are bivalent iron and magnesium, and trivalent chromium, aluminum, and iron, the general formula being (Mg, Fe)O·(Cr, Al, Fe)$_2$O$_3$. The end members ferrochromite (FeO·Cr$_2$O$_3$), magnesiochromite (MgO·Cr$_2$O$_3$), spinel (MgO·Al$_2$O$_3$), hercynite (FeO·Al$_2$O$_3$), magnesioferrite (MgO·Fe$_2$O$_3$) and magnetite (FeO·Fe$_2$O$_3$) occupy the corners of a triangular prism of composition. The principal zone of isomorphism for the chromites in the triangular prism of composition ranges from compositions approaching magnesiochromite and spinel to magnetite, leading to the division of chromites into the following types, with the replaceable ions written in order of abundance: aluminian chromite (Mg, Fe)O·(Cr, Al, Fe)$_2$O$_3$; ferrian chromite (Mg, Fe)O·(Cr, Fe, Al)$_2$O$_3$; chromian spinel (Mg, Fe)O·(Al, Cr, Fe)$_2$O$_3$; ferrian spinel (Mg, Fe)O·(Al, Fe, Cr)$_2$O$_3$; chromian magnetite (Fe, Mg)O·(Fe, Cr, Al)$_2$O$_3$; and aluminian magnetite (Fe, Mg)O·(Fe, Al, Cr)$_2$O$_3$. The analyses may also be calculated to four-end members; however, several groups of four-end members may be selected to interpret one analysis and no single group of four-end members suffices for all of the analyses.

---

* Published by permission of the Director, U. S. Geological Survey, Department of the Interior, Washington, D. C.

INTRODUCTION

Since 1939 the Geological Survey, U. S. Department of the Interior, has been studying domestic deposits of chromite as part of its Strategic Minerals Program and, beginning in 1940, has examined some chromite deposits in Latin America with the help of funds allocated by the State Department. As part of these investigations 52 complete chemical analyses and partial chemical analyses of chromite have been made in the chemical laboratory of the Geological Survey. Many of the analyses

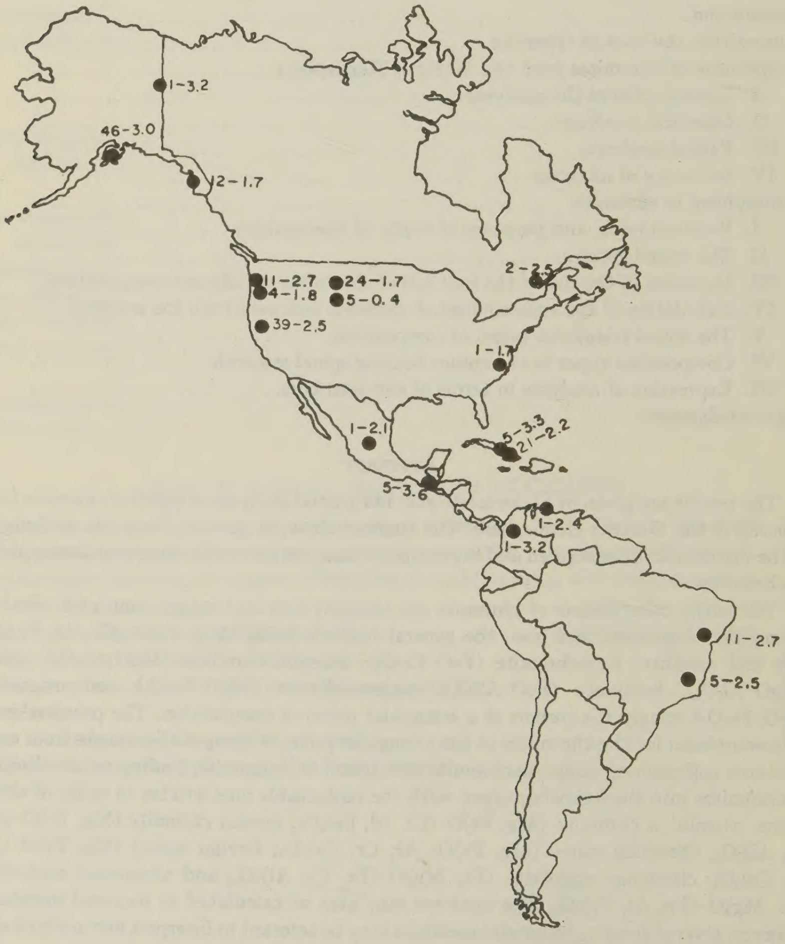

FIG. 1. Distribution, number and grade of chromites analyzed. The first figure at each locality is the number of samples analyzed, the second figure the average ratio of Cr to Fe in the chromites.

have been published in Strategic Minerals Bulletins of the Survey, and others will be cited in forthcoming issues.

The purpose of this report is: (1) to discuss briefly our present concept of the composition of the mineral chromite as revealed by these analyses, and (2) to outline the methods of study of chromite used in the Geological Survey Laboratory. The locations of the areas from which samples have been taken are shown on the outline map of the Western Hemisphere, Fig. 1. These samples have been collected in the field by the Federal geologist studying the particular deposit or area.

COMPOSITION AND USES OF CHROMITE

The composition of chromite is so variable that chrome ore consisting entirely of the mineral chromite may have a Cr_2O_3 content of less than 30% or of more than 60%, and the ore may or may not meet requirements for a particular grade. On the other hand, in ore containing little chromite the purified mineral may be of sufficiently high chromium content for metallurgical use.

The chemical composition of a chromite shows, in general, the use for which it is suitable. Chromite of metallurgical grade is generally considered to be that having three parts by weight of chromium to one of total iron. From chromite of this composition is produced ferrochromium, containing 60 to 70 per cent chromium, which is added to the steel to make alloys of any chromium content desired. According to Ridgway and Melcher[1] " . . . the steel industry is charged with three-fourths of the domestic consumption." Most of this is used in making alloys, although a large part is used for refractory furnace lining. More recently lower grades of chromite have been used for metallurgical purposes by eliminating the intermediate step of producing ferrochromium, and " . . . one domestic concern," according to Ridgway and Melcher, "makes chromium-alloy steels in the electric furnace directly from alloy steel scrap, mild steel scrap, and chromite."

Refractory and chemical grades of chromite need not have as high a chromium content as metallurgical grades. However, certain physical and chemical properties are needed for a good refractory. The Cuban ores, which have only a moderate content of chromium, but a relatively high alumina content (with a rather low content of iron), are much used as refractories. The main requirement of chromite for chemical use is that its chromium content be sufficiently high to make worth while conversion to chromates and dichromates.

---

[1] Ridgway, R. H., and Melcher, N. B., Chromite: *U. S. Bureau of Mines Minerals Yearbook*, Review of **1940**, 585–596 (1941).

Chromite is a member of the spinel group of minerals and, like other members of the group, should approximate the composition of the general formula $R''R_2'''O_4$ or $RO \cdot R_2O_3$, where RO represents oxides of bivalent metals (chiefly Fe″, Mg) and R_2O_3 oxides of trivalent metals (chiefly Cr, Fe‴, Al).

In the absence of a satisfactory method of determining ferrous oxide in chromite, some uncertainty existed as to whether or not chromite has a 1 to 1 ratio of RO to R_2O_3, as do other members of the spinel group. In many earlier analyses of chromite ferrous oxide was calculated from the total iron content so as to give the spinel formula, or else all of the iron was reported as FeO.

A method for determining ferrous oxide in chromite using phosphoric acid as a solvent in the absence of air was devised by Konopicky and Caesar.[2] Their analyses of a number of chrome ores showed RO to R_2O_3 ratios approaching but generally less than 1:1, after subtracting impurities.

Of the 52 complete analyses given in this paper, ferrous oxide was determined in 41 samples by a modification of the Konopicky and Caesar method. Of these, 31 samples show a ratio of RO to R_2O_3 of 1:1 within experimental error (.95 to 1.05), and in ten other samples the ratio is appreciably less than 1:1. The deficiency of RO to R_2O_3 in some samples was considered due to alteration (oxidation of ferrous to ferric oxide), as many of the abnormal chromites had a dull luster and tiny opaque inclusions could be seen with the microscope.

COMPOSITION OF CHROMITES FROM THE WESTERN HEMISPHERE

I. General plan of the analyses

The plan of the analytical work was such as to reveal the composition of the chromite as well as the percentage of it in the ore. The quantity of gangue impurities was reduced in general to less than one per cent by means of heavy-solution separations.

In the complete analyses of the chromite concentrates five major constituents were determined: Cr_2O_3, Al_2O_3, Fe_2O_3, FeO, and MgO. In addition five minor constituents were determined: MnO, CaO, TiO_2, SiO_2, and H_2O+. Determinations of trace elements such as vanadium, nickel, and zinc were not generally made. Phosphorus and sulphur, if present at all, were assumed to be present in the gangue and their determination in purified chromite seemed unnecessary. In the partial analyses only iron and chromium were determined in the chromite concentrate.

---

[2] Konopicky, K., and Caesar, F., Determination of FeO in chrome ore: *Ber. deut. keram. Ges.*, **20**, 362 (1939).

Scheme of Analysis of Chromite

Fuse 0.5 gram chromite with 4 grams Na_2CO_3 and 0.4 gram KNO_3. Cool, let stand over night in 75 ml. H_2O. Filter, wash with 0.1 per cent Na_2CO_3 solution.

<table>
<tr><td colspan="2">Filtrate: Na_2CrO_4, $NaAlO_2$, Na_2SiO_3. Add excess of H_2SO_4, neutralize with NH_4OH, filter. Redissolve ppt. in H_2SO_4, reprecipitate with NH_4OH, filter.</td><td colspan="2">Residue: Contains Fe, Ti, Mg, Mn, Ca with some alumina and silica. Dissolve in dilute HCl, neutralize with NH_4OH, filter.</td></tr>
<tr><td rowspan="3">Combined filtrates: Na_2CrO_4. Titrate with $FeSO_4$ and $KMnO_4$</td><td>Precipitate: Hydroxides of Al, Si.</td><td>Precipitate: Hydroxides of Fe, Ti, Al, Si with traces of Mg, Mn and Ca.</td><td rowspan="2">Filtrate: Chlorides of Mg, Mn, Ca.</td></tr>
<tr><td colspan="2">Combine, dissolve in dilute HNO_3, neutralize with NH_4OH, filter</td></tr>
<tr><td>Precipitate: Hydroxides of Fe, Al, Ti, Si. Ignite and weigh as oxides. Determine SiO_2, TiO_2, Fe_2O_3; obtain Al_2O_3 by difference.</td><td>Filtrate: Nitrates of Mg, Mn, Ca. Combine. Weigh Mg, Mn, Ca as pyrophosphates. Determine CaO and MnO; MgO by difference.</td><td></td></tr>
</table>

Chromium alone was determined in the ore and the percentage of chromite in the ore was obtained by dividing the chromium content of the ore by that of the concentrate. The content of chromite in the ore was reported only to whole percentages as small errors were caused by incomplete purification of the separated chromite and the possible presence of a small quantity of chromium in gangue minerals. As one of these errors is plus and the other minus, no corrections were made even when the percentage of residual gangue was known as in the complete analyses.

II. Complete analyses

In Table 1 are listed 52 complete analyses of chromite and chromium-bearing spinel minerals from the Western Hemisphere. The wide range in composition can readily be seen. None of the samples has a composition near that of the ferrochromite end member, $FeO \cdot Cr_2O_3$, the formula usually assigned to chromite.

Samples 22 to 30 were the first analyzed by the writer and were analyzed according to the usual methods of rock analysis as described by Hillebrand and Lundell,[3] methods not particularly suitable for chromite. These analyses are reported to tenths of a per cent only, to show that inaccuracies are involved. Among these samples are chromium-bearing magnetites and spinels and their consideration helps in showing the trend of isomorphism in chromite.

---

[3] Hillebrand, W. F., and Lundell, G. E. F., *Applied Inorganic Analysis*, John Wiley & Sons, Inc., New York (1929).

Sample 32 was analyzed by Dr. Roger C. Wells, Chief Chemist of the Geological Survey, using the method of the writer.

The general scheme of analysis used is shown in tabular outline (Scheme of Analysis of Chromite). In addition ferrous oxide was determined by a closed tube modification of the method of Konopicky and Caesar[4] and water was determined by the Penfield tube method.

TABLE 1. ANALYSES OF CHROMITE AND RELATED MINERALS

1–5. Kenai Peninsula, Alaska.

2. Red Mountain, Kenai Peninsula, Alaska. Chromite from recrystallized ore, deposit no. 1. Analysis quoted and geologic occurrence described in *U. S. Geol. Survey, Bull.* **931-G**, pp. 151–152 and 165 (1941). Collected by Philip Guild.
3. Red Mountain, Kenai Peninsula, Alaska. Chromite from normal ore, from unaltered inclusion in dike, deposit no. 1. *op. cit.*, pp. 151–152 and 165. Collected by Philip Guild.
4. Red Mountain, Kenai Peninsula, Alaska. Chromite from high-grade ore, deposit no. 10, *op. cit.*, pp. 151–152 and 170. Collected by Philip Guild.
5. Claim Point, Kenai Peninsula, Alaska. Chromite from high-grade ore, deposit no. 6. *op. cit.*, pp. 151–152 and 160. Collected by Philip Guild.

Sample no.	1	2	3	4	5
Cr_2O_3	31.31	34.81	57.83	48.55	48.45
Al_2O_3	16.59	22.93	9.90	15.83	14.43
Fe_2O_3	18.24	10.83	4.05	7.31	6.97
FeO	23.94	21.24	14.98	16.11	17.67
MgO	7.78	9.74	12.55	11.78	11.03
MnO	.32	.22	.20	.18	.24
CaO	.14	.06	.06	.10	.16
TiO_2	1.44	.56	.16	.44	.48
SiO_2	.30	.08	.36	.10	.34
H_2O+	—	—	—	—	—
	100.06	100.47	100.09	100.40	99.77
Cr	21.42	23.82	39.59	33.22	33.16
Fe	31.37	24.09	14.48	17.64	18.62
Ratio Cr/Fe	.68	.99	2.73	1.88	1.78
Impurity	olivine	olivine	olivine	olivine	olivine
Ratio RO/R_2O_3*	1.05	1.01	1.02	.99	1.01
Cr_2O_3 in ore	—	34.3	43.4	47.4	46.9
% Chromite in ore	—	99	75	98	97

* After subtracting ilmenite and the silicate impurity.

---

[4] Konopicky, K., and Caesar, F., Determination of FeO in chrome ore: *Ber. deut. keram. Ges.*, **20**, 362 (1939).

6. Pillikin mine, Sec. 28, T. 11 N., R. 8 E., Eldorado County, California. Disseminated chromite ore from Shovel pit area no. 3, West Basin. Location shown on plates 66 and 69 and descriptions given pp. 447-450, *U. S. Geol. Survey, Bull.* **922-P.** Collected by F. G. Wells, 1940.
7. Pillikin mine, Sec. 28, T. 11 N., R. 8 E., Eldorado County, California. Massive ore from Shovel pit area no. 3, West Basin, idem. Collected by F. G. Wells, 1940.
8. Pillikin mine, Sec. 28, T. 11 N., R. 8 E., Eldorado County, California. Fine grained disseminated ore from pit on right side of road into area 4, Chrome Gulch, NW ¼ of SW ¼ of Sec. 21. Location shown on plate 66 and described on page 451. Op. cit. Collected by F. G. Wells, 1940.
9. Coggins mine, Sec. 35, T. 39 N., R. 4 W., Little Castle Creek, Shasta County, California. Leopard ore, aggregates of chromite nodules in dunite. From dump Coggins mine. Collected by F. G. Wells, 1940.
10. Pick and Shovel mine, Sec. 34, 35, T. 29 S., R. 12 E., San Luis Obispo County, California. Massive ore from pod type of deposit. Collected by C. T. Smith, 1940.

Sample no.	6	7	8	9	10
Cr_2O_3	52.77	55.84	54.45	52.18	55.42
Al_2O_3	10.31	10.75	7.90	10.80	12.61
Fe_2O_3	9.99	6.19	7.90	4.53	8.10
FeO	12.40	12.49	15.34	20.67	8.19
MgO	12.10	13.54	12.60	9.58	13.70
MnO	.32	.27	.27	.32	.16
CaO	.16	.16	.06	.10	.16
TiO_2	.17	.18	.23	.26	.13
SiO_2	.92	.52	.90	.88	.90
H_2O+	.76	.40	.38	.40	.48
	99.90	100.34	100.03	99.72	99.85
Cr	36.09	38.21	37.27	37.08	37.93
Fe	16.61	14.04	17.45	19.22	12.02
Ratio Cr/Fe	2.17	2.72	2.14	1.93	3.16
Impurity	olivine	serpentine	serpentine	olivine	serpentine
Ratio RO/R_2O_3*	.88	.98	1.04	1.05	.80
Cr_2O_3 in ore	16.3	45.3	34.1	17.8	48.1
% chromite in ore	31	81	63	34	87

* After subtracting ilmenite and the silicate impurity.

11. Sweetwater mine, Sec. 11, 12., T. 29 S., R. 11 E., San Luis Obispo County, California. Massive chromite ore, collected by C. T. Smith, 1940.
12. Castro mine, Sec. 29, T. 29 S., R. 12 E., San Luis Obispo County, California. Disseminated chromite ore, collected by C. T. Smith, 1940.
13. Black Diamond Claims, Sec. 25, T. 22 N., R. 7 W., Glenn County, California. Disseminated ore. Grab sample taken across 30′ width of ore 25′ NW of the most southern pit. Collected by D. P. Wheeler, Jr., 1940.
14. Black Diamond Claims, Sec. 25, T. 22 N., R. 7 W., Glenn County, California. Disseminated ore. Sample cut across 12 ft. of ore on the south wall of upper pit. Collected by D. P. Wheeler, Jr., 1940.

Sample no.	11	12	13	14
Cr_2O_3	50.99	47.57	56.98	56.75
Al_2O_3	16.21	18.61	11.03	9.93
Fe_2O_3	3.44	4.80	4.81	6.03
FeO	14.65	13.06	11.40	12.94
MgO	13.40	13.91	14.55	13.00
MnO	.23	.14	.16	.16
CaO	.14	.24	.14	.24
TiO_2	.17	.13	.18	.22
SiO_2	.42	.86	.40	.40
H_2O+	.34	.54	.20	.15
	99.99	99.86	99.85	99.82
Cr	34.89	32.53	38.98	38.82
Fe	13.80	13.51	12.22	14.28
Ratio Cr/Fe	2.53	2.41	3.19	2.72
Impurity	serpentine	serpentine	serpentine	serpentine
Ratio RO/R_2O_3*	1.03	.97	1.00	.97
Cr_2O_3 in ore	42.8	30.8	37.4	16.4
% chromite in ore	84	65	66	29

* After subtracting ilmenite and the silicate impurity.

15. Northern pit of Veta Chica deposit, McGuffy Creek, Sec. 30, T. 45 N., R. 10 W., Siskiyou County, California. Collected by J. S. Livermore.
16. Southern end of Cerro Colorado claim, McGuffy Creek, Sec. 25, T. 45 N., R. 11 W., Siskiyou County, California. Collected by J. S. Livermore.
17. From Veta Grande claim, McGuffy Creek, Sec. 30, T. 45 N., R. 10 W., Siskiyou County, California. Collected by J. S. Livermore.
18. Anhedral chromite in fresh dunite from cut on Ribbon claim, at altitude of about 4000 feet, west of Green Creek, Twin Sisters Mountains, Washington. Collected by T. P. Thayer.
19. Massive chromite from Danny deposit, at altitude of about 3600 feet, in south wall of glacial cirque at head of South Fork of the Nooksack River, Twin Sisters Mountains, Washington. Collected by T. P. Thayer.

Sample no.	15	16	17	18	19
Cr_2O_3	58.45	55.30	56.83	59.40	58.80
Al_2O_3	9.36	11.51	9.27	10.28	9.66
Fe_2O_3	4.47[a]	4.67[a]	5.19[a]	3.30	3.10
FeO	14.15[a]	15.58[a]	17.19[a]	14.09	13.88
MgO	12.71	12.06	10.77	12.62	12.96
MnO	.12	.22	.22	.14	.12
CaO	None	.08	None	.14	.16
TiO_2	.33	.41	.26	.14	.06
SiO_2	.22	.32	.34	.12	.10
H_2O+	.08	.12	Trace	—	—
	99.89	100.27	100.07	100.24	98.84
Cr	40.01	37.85	38.90	40.67	40.25
Fe	14.14	15.39	16.99	13.26	12.95
Ratio Cr/Fe	2.83	2.46	2.29	3.07	3.11
Impurity	—	—	—	olivine	olivine
Ratio RO/R_2O_3*	—	—	—	.99	1.03
Cr_2O_3 in ore	41.39	39.90	17.40	51.2	52.8
% chromite in ore	71	72	31	86	87

* After subtracting ilmenite and the silicate impurity.

[a] Calculated to give 1 to 1 ratio of RO to R_2O_3.

20. Leader claim, Twin Sisters Range, Washington. Sec. 4, T. 36 N., R. 7 E.
21. Leader claim, Twin Sisters Range, Washington. Sec. 4, T. 36 N., R. 7 E.
22. Specimen 2 feet from south contact of southwest ore body, Chambers mine, Grant County, Oregon, described on pp. 96–98, *U. S. Geol. Survey, Bull.* **922-D.** Collected by T. P. Thayer, 1940.
23. Specimen taken 17 feet north of No. 22, near center of same ore body. Collected by T. P. Thayer, 1940.
24. Big Bertha mine, Grant County, Oregon. Location shown on Plate 13, and deposit described on pp. 108, 109, *U. S. Geol. Survey, Bull.* **922-D.** Collected by T. P. Thayer, 1940.

Sample no.	20	21	22	23	24
Cr_2O_3	56.25	55.71	35.4	37.5	32.2
Al_2O_3	10.52	10.93	28.3	28.9	32.0
Fe_2O_3	5.34[a]	5.27[a]	5.5	3.9	5.6
FeO	15.97[a]	15.69[a]	13.6	12.7	12.6
MgO	11.66	12.07	15.3	15.8	15.7
MnO	.22	.20	.1	.1	.1
CaO	None	.02	.1	.1	.1
TiO_2	.19	.23	.3	.2	.3
SiO_2	.18	.20	.3	.2	.2
H_2O+	Trace	Trace	.4	None	.1
	100.33	100.32	99.3	99.4	98.9
Cr	38.50	38.12	24.2	25.7	22.0
Fe	16.16	15.90	14.4	12.5	12.7
Ratio Cr/Fe	2.38	2.40	1.68	2.06	1.73
Impurity	—	—	olivine	olivine	olivine
Ratio RO/R_2O_3*	—	—	1.02	1.01	.99
Cr_2O_3 in ore	24.38	15.46	20.0	28.1	26.5
% Chromite in ore	43	28	57	75	82

* After subtracting ilmenite and the silicate impurity.

[a] Calculated to give 1 to 1 ratio of RO to R_2O_3.

25. Silver Lease mine, Sec. 17, T. 13 S., R. 31 E., Grant County, Oregon. Deposit described on p. 110, *U. S. Geol. Survey, Bull.* **922-D.** Collected by T. P. Thayer, 1940.

26–30. Casper Mountain, Natrona County, Wyoming. Collected by E. L. and H. K. Stephenson.

Sample no.	25	26	27	28	29	30
Cr_2O_3	35.5	25.4	42.7	13.7	18.4	28.2
Al_2O_3	26.2	4.7	10.1	3.4	2.8	2.7
Fe_2O_3	7.9	46.3	16.1	53.0	45.6	36.5
FeO	12.4	17.5	24.9	27.4	25.6	27.9
MgO	15.2	1.6	4.1	1.2	1.2	2.3
MnO	.1	.5	.4	.2	.2	.2
CaO	.1	.3	.3	.3	.3	.3
TiO_2	.3	3.0	.6	.5	2.9	1.0
SiO_2	.2	.8	.4	.3	.8	.2
H_2O+	1.3	—	—	—	—	—
	99.2	100.1	99.6	100.0	97.8	99.3
Cr	24.3	17.4	29.2	9.4	12.6	19.3
Fe	15.1	46.0	31.1	58.4	51.8	47.2
Ratio Cr/Fe	1.61	.38	.94	.16	.24	.41
Impurity	olivine	serpentine	serpentine	serpentine	serpentine	serpentine
Ratio RO/R_2O_3*	1.00	.47	.92	.89	.78	.86
Cr_2O_3 in ore	28.9	—	—	—	—	—
% Chromite in ore	81	—	—	—	—	—

* After subtracting ilmenite and the silicate impurity.

31. Little Rocky Creek, Stillwater Complex, Stillwater County, Montana. Chromite from massive one-foot layer 150 feet above the base of the complex, 100 feet west of Little Rocky Creek. For geologic map of area see Plate 63, *U. S. Geol. Survey, Bull.* **922-N.** Collected by J. W. Peoples, 1940.
32. Ledge west of Mt. View lake, Stillwater complex, Stillwater County, Montana. Analysis by R. C. Wells using author's procedure. Chromite from massive lowest layer of the lower or *G* zone. For geologic occurrence of this chromite see *U. S. Geol. Survey, Bull.* **922-N,** p. 415–416 and Plate 63 (1940). Collected by J. W. Peoples, 1940.
33. Bobcat Creek Cirque, East Boulder Plateau, Stillwater complex, Sweetgrass County, Montana. Chromite from 2.5-foot layer occurring about 250 feet stratigraphically above the base of the complex. Collected by A. L. Howland, 1942.
34. Champion No. 3 claim, East Boulder Plateau, Stillwater complex, Sweetgrass County, Montana. Chromite from top of one-foot layer near the center of the Ultramafic Zone of the complex. The ore is magnetic. Collected by A. L. Howland, 1941.
35. Raise in Drift No. 2, Benbow mine, Stillwater County, Montana. Massive ore from near middle of Ultramafic Zone. For geologic description of area see *U. S. Geol. Survey, Bull.* **922-N,** pp. 371–413. Collected by J. W. Peoples, 1941.

Sample no.	31	32	33	34	35
Cr_2O_3	43.71	46.20	43.84	45.62	45.79
Al_2O_3	17.34	15.60	18.36	19.16	17.20
Fe_2O_3	7.22	8.46[a]	6.45[a]	5.05[a]	7.69
V_2O_3	—	—	—	—	Trace
FeO	19.27	16.66[a]	20.66[a]	18.64[a]	17.16
MgO	11.00	11.67	9.38	10.75	11.61
MnO	.21	.01	.21	.18	.19
CaO	.34	.28	.08	.02	.02
NiO	—	.12	—	—	—
TiO_2	.79	.72	.79	.44	.40
SiO_2	.34	.32	.24	.20	.14
H_2O+	.08	—	.02	.06	.08
	100.30	100.04	100.03	100.12	100.28
Cr	29.91	31.62	30.00	31.22	31.31
Fe	20.02	18.88	20.55	17.99	18.70
Ratio Cr/Fe	1.49	1.67	1.46	1.74	1.68
Impurity	pyroxene	—	serpentine	serpentine	serpentine
Ratio RO/R_2O_3*	1.06	—	—	—	1.01
Cr_2O_3 in ore	—	42.32	32.94	42.50	34.58
% Chromite in ore	—	92	75	93	76

* After subtracting ilmenite and silicate impurity.

[a] Calculated from total iron to give 1 to 1 ratio of RO to R_2O_3.

36. Gish property, Boulder River, Stillwater County, Montana. Massive ore from base of main chromite layer, near middle of Ultramafic Zone. Collected by J. W. Peoples, 1941.
37. Mountain View Lake Area, Stillwater Complex, Stillwater County, Montana. Spotted ore from upper part of upper or *H* chromite zone. For general geologic description of area see *U. S. Geol. Survey, Bull.* **922-N**, pp. 415–416 and Plate 64. Collected by J. W. Peoples.
38. Mountain View Lake Area, Stillwater Complex, Stillwater County, Montana. Massive ore from lower part of *H* zone. Collected by J. W. Peoples.
39. Aventura mine, Camaguey Province, Cuba. Analyses quoted and geology described in *U. S. Geol. Survey, Bull.* **935-A.** Collected by T. P. Thayer.
40. Guillermina mine, Camaguey Province, Cuba. Analysis quoted and geology described in *U. S. Geol. Survey, Bull.* **935-A.** Collected by T. P. Thayer.

Sample no.	36	37	38	39	40
Cr_2O_3	46.02	44.44	47.82	35.21	35.60
Al_2O_3	19.38	18.60	16.90	32.21	30.37
Fe_2O_3	3.87	6.53	5.30	2.83	3.65
V_2O_3	Trace	—	.04	—	—
FeO	18.38	18.01	16.45	12.11	13.04
MgO	11.19	11.16	12.11	16.89	16.14
MnO	.18	.18	.16	.13	.15
CaO	.04	.02	.04	.28	.28
TiO_2	.50	.47	.43	.31	.63
SiO_2	.28	.18	.22	.24	.52
H_2O+	.16	.02	.26	Trace	Trace
	100.00	99.61	99.73	100.21	100.38
Cr	31.48	30.38	32.71	24.10	24.37
Fe	16.96	18.55	16.48	11.39	12.68
Ratio Cr/Fe	1.86	1.64	1.99	2.12	1.92
Impurity	serpentine	olivine	olivine	mixture	labradorite
Ratio RO/R_2O_3*	1.01	1.01	1.01	1.04[a]	1.05
Cr_2O_3 in ore	40.72	22.24	36.32	—	—
% chromite in ore	89	50	76	—	—

* After subtracting ilmenite and the silicate impurity.

[a] Not corrected for silicate impurity.

41. Clemencia mine, Holguin district, Cuba. Analysis quoted and geology described in *U. S. Geol. Survey, Bull.* **935-A,** 1942. Collected by T. P. Thayer.
42. Caledonia mine, Mayari district, Cuba. Analysis quoted and geology described *op. cit.* Collected by T. P. Thayer.
43. Carnesoltas mine, Camaguey, Cuba. Analysis quoted and geology described *op. cit.* Collected by T. P. Thayer.
44. La Paz mine, Jalapa, Guatemala. Collected by W. D. Johnston, Jr.
45. Esperanza Hill, Jalapa, Guatemala. Collected by W. D. Johnston, Jr.

Sample no.	41	42	43	44	45
Cr_2O_3	41.78	56.89	22.31	60.26	61.10
Al_2O_3	26.70	13.77	44.73	8.87	8.40
Fe_2O_3	3.16	1.27	7.04	3.64[a]	4.31[a]
FeO	11.33	13.44	7.22	12.37[a]	10.56[a]
MgO	16.15	14.42	17.04	13.90	14.86
MnO	.11	.17	.16	.10	.15
CaO	.14	.12	.14	.10	.10
TiO_2	.31	.13	.20	.14	.11
SiO_2	.68	.32	.60	.50	.28
H_2O+	Trace	Trace	.86	.22	.04
	100.36	100.53	100.30	100.00	99.91
Cr	28.59	38.93	15.26	41.24	41.81
Fe	11.01	11.34	10.53	12.12	11.20
Ratio Cr/Fe	2.60	3.44	1.45	3.40	3.73
Impurity	serpentine	serpentine	serpentine	serpentine	serpentine
Ratio RO/R_2O_3*	.98	1.04	.81	—	—
Cr_2O_3 in ore	—	—	—	56.67	59.40
% Chromite in ore	—	—	—	94	97

* After subtracting ilmenite and the silicate impurity.

[a] Calculated from total iron to give 1 to 1 ratio of RO to R_2O_3.

46. La Carona mine, Jalapa, Guatemala. Collected by W. D. Johnston, Jr.
47. State of Falcon, Venezuela. Collected by W. D. Johnston, Jr.
48. Cascabulhos mine, Baia, Brazil. Collected by W. D. Johnston, Jr.
49. Campinhos mine, Baia, Brazil. Collected by W. D. Johnston, Jr.
50. Pedrinhas mine, Baia, Brazil. Collected by W. D. Johnston, Jr.

Sample no.	46	47	48	49	50
Cr_2O_3	56.15	41.63	56.24	58.18	58.60
Al_2O_3	13.87	25.20	12.42	11.30	11.08
Fe_2O_3	2.26[a]	3.38	4.44	3.46	3.94
FeO	12.30[a]	12.29	12.72	13.28	12.06
MgO	14.40	16.19	12.47	12.89	13.57
MnO	.16	.13	.37	.25	.13
CaO	.06	.16	.12	.06	.04
TiO_2	.05	.30	.21	.15	.19
SiO_2	.46	.36	.38	.22	.22
H_2O+	.26	.24	.44	.26	.26
	99.97	99.88	99.81	100.05	100.11
Cr	38.41	28.50	38.50	39.80	40.10
Fe	11.13	11.90	13.00	12.74	12.13
Ratio Cr/Fe	3.45	2.40	2.98	3.12	3.31
Impurity	serpentine	serpentine	serpentine	serpentine	serpentine
Ratio RO/R_2O_3*	—	1.02	.93	.97	.95
Cr_2O_3 in ore	51.77	34.21	48.08	53.01	52.24
% Chromite in ore	92	82	86	91	89

* After subtracting ilmenite and the silicate impurity.

[a] Calculated from total iron to give 1 to 1 ratio of RO to R_2O_3.

51. Santa Luzia, Baia, Brazil. Collected by W. D. Johnston, Jr.
52. Piûi, Minas Geraes, Brazil. Collected by W. D. Johnston, Jr.

Sample no.	51	52
Cr_2O_3	49.20	52.60
Al_2O_3	19.10	13.12
Fe_2O_3	6.76	6.65
FeO	9.36	11.57
MgO	14.41	14.03
MnO	.14	.28
CaO	.14	.14
TiO_2	.26	.39
SiO_2	.24	.36
H_2O+	.20	.56
	99.81	99.70
Cr	33.68	36.00
Fe	12.00	13.64
Ratio Cr/Fe	2.81	2.64
Impurity	olivine	serpentine
Ratio RO/R_2O_3*	.87	.97
Cr_2O_3 in ore	43.88	50.70
% Chromite in ore	89	96

* After subtracting ilmenite and the silicate impurity.

III. Partial Analyses

In Table 2 are given partial analyses of chromite. These include analyses of the chromite concentrate for chromium and iron and of the ore for chromium alone, and calculation of the ratio of chromium to iron in the concentrate and of the percentage of chromite in the ore.

TABLE 2. PARTIAL ANALYSES OF CHROMITE.

Location of samples.

53. Ten miles south of Eagle, Alaska. Collected by J. B. Mertie, Jr.

54–94. Claim Point, near Seldovia, Kenai Peninsula, Alaska. Collected by P. W. Guild. Geology described in *U. S. Geological Survey, Bull.* **931–G,** pp. 139–175 (1941).
74. Deposit 24, Red Mtn., represents 1.5 ft. of ore from middle band of three, 110 ft. S.E. of the N.W. end of deposit.
75. Deposit 24, Red Mtn., represents 3.8 ft. of ore from the middle band.
76. Deposit 8, the patented Juneau No. 1 claim, Red Mtn., 53 ft. N.W. of discovery trench, represents 4.8 ft. of ore from the S. contact to center of the body.
77. Same as 76, but represents 4.6 ft. of ore from N. end of 76 to the N. contact of the ore.
78. Deposit 11, Red Mtn., from shallow trench on E. crest of ridge. Represents 4.0 ft. of ore measured from the S. contact of the body.

79. Same as 78, but represents 2.6 ft. directly N. of 78.
80. Same as 78, but represents 4.5 ft. of low grade ore beginning 4 ft. N. of 78.
81. Deposit 11, Red Mtn., 36 ft. E. of crest of ridge. Represents 6.8 ft. of ore.
82. Deposit 2, on patented Star No. 4 claim, Red Mtn., from S. edge of the discovery shaft. Lowest ore band, 1.3 ft. thick.
83. Same as 82, but represents 3.5 ft. of ore above 82.
84. Same as 82, but represents 4.2 ft. of ore above 83.
85. Same as 82, but 250 ft. N. of discovery shaft; represents 1.1 ft. from lower band.
86. Same as 85, but represents 2.8 ft. from upper band.
87. Deposit 12, Red Mtn., represents 2.6 ft. of ore at the discovery monument, midway between the ends of the deposit.
88. Depost 27, Red Mtn., represents 5.0 ft. of disseminated ore from the low grade body 75 ft. N.E. of discovery monument.
89. Deposit 28, Red Mtn., represents 4.0 ft. of ore at center of deposit.
90. Star No. 4 deposit, 350 ft. N. of discovery shaft. Represents 2.1 ft. of low grade ore from lowest band.
91. Same as 90, but represents 1.4 ft. from next high band.
92. Same as 91, but represents 1.1 ft. from next high band.
93. Same as 92, but represents 1.3 ft. from topmost band.
94. Deposit 20, Red Mtn., represents 2.1 ft. of disseminated ore taken 5 ft. above the prominent fault near base of outcrop.

95-98. Red Bluff Bay, Alaska. Collected by J. R. Balsley, 1941. Geology described in *U. S. Geological Survey, Bull.* **936–G,** pp. 171–187.
95. From deposit No. 3.
96. From high grade lens deposit No. 8.
97. From deposit No. 7.
98. From deposit No. 5.
99–106. Red Bluff Bay, Alaska. Collected by P. W. Guild, 1941. Geology described in *U. S. Geol. Survey, Bull.* **936–G,** pp. 171–187.
99. From narrow chromite layers 1,000 feet west-northwest of deposit No. 3.
100. From chromite lens 500 feet northwest of deposit No. 3.
101. From deposit No. 4.
102. From south end of deposit No. 6.
103. From north end of deposit No. 6.
104. From north lens of deposit No. 2.
105. From south end of deposit No. 1.
106. From north end of deposit No. 1.

107–113. Twin Sisters Mountains, Washington.
107. High-grade band, Meadows claim. Collected by T. P. Thayer.
108. Whistler claim. Collected by T. P. Thayer.
109. Ted claim. Collected by T. P. Thayer.
110. McMaster claim. Collected by T. P. Thayer.
111. Galbraith claim. Collected by T. P. Thayer.
112. Middle of Meadows claim (Sec. 3, T. 36 N., R. 7 E.). Collected by F. G. Wells.
113. Meadows claim. Collected by F. G. Wells.
114–125. San Luis Obispo County, Calif. Collected by F. G. Wells.
114. Pick & Shovel mine. Sec. 34, T. 29 S., R. 12 E.
115. Pick & Shovel mine. Sec. 34, T. 29 S., R. 12 E.
116. Sweetwater mine. Sec. 12, T. 29 S., R. 11 E.

117. Sweetwater mine.
118. Eucalytus No. 1 claim.
119. Seeley property. Sec. 34, T. 29 S., R. 12 E.
126–129. McGuffy Creek, Sec. 30, T. 45 N., R. 10 W., Sec. 25, T. 45 N., R. 11 W., Siskiyou County, California. Collected by J. S. Livermore.
126. S.W. pit on ore zone extending through southern half of Grand Falls claim and northern half of Grand Canyon claim.
127. N.W. pit of Cerro Colorado claim.
128. Weeks claim, north of McGuffy Creek.
129. Mary Lou (Octopus) claim.
130–133. Pillikin mine, Sec. 28, T. 11 N., R. 6 E., Eldorado County, California. Collected by F. G. Wells. Geology of the chromite deposits described in *U. S. Geological Survey, Bull.* **922–O,** pp. 417–460 (1940).
130. Massive chromite from Chrome Gulch.
131. Pit No. 5A.
132. Low grade ore from pit No. 5A.
133. Disseminated ore from south end of pit No. 6.
134–135. Black Diamond claims, Sec. 25, T. 22 N., R. 7 W., Glenn County, California. Collected by F. G. Wells.
136–140. Stanislaus County, California. Collected by F. G. Wells.
136. Black Bart claim, Sec. 16, T. 6 S., R. 5 E.
137. Adobe Canyon; grab samples from sacks awaiting shipment. Sec. 14, T. 6 S., R. 5 E.
138. West Black Bart mine, grab sample from ore pile. Sec. 16, T. 6 S., R. 5 E.
139. West Black Bart mine, grab sample from ore pile.
140. No. 5 property, Sec. 15, T. 6 S., R. 5 E.

141–155. Stillwater Area, Montana. Sample 141 collected by A. L. Howland; the others by J. W. Peoples. Geology of the eastern part of the chromite bearing belt described in *U. S. Geological Survey, Bull.* **922–N,** pp. 371–415 (1940).
141. Bottom of 1 ft. chromite layer, 20 feet N. of discovery pit of Champion No. 3 claim, East Boulder Plateau.
142. Massive chromite 3.6 feeet above base of "*G*" Zone, Mountain View Lake area.
143. Massive chromite 5.3 feet above base of "*G*" Zone, Mountain View Lake area.
144. Disseminated chromite, 4.4 feet above the base of the "*G*" Zone, Montain View Lake area.
145. Massive chromite, 7.4 feet above the base of the "*G*" Zone.
146. Top layer of "*G*" Zone, Mountain View Lake area.
147. Hanging wall chromite layer from portal of No. 4 Adit, Monat mine.
148. Spotted ore from Nye Basin.
149. Hanging Wall chromite layer above "*G*" Zone, Montain View Lake area.
150. Massive ore from Discovery pit of Sunshine claim, West Fork of Stillwater River.
151. Massive ore from 1 foot layer, Sunshine claim, West Fork of Stillwater River.
152. Typical ore from Ground Hog claim, West Fork of Stillwater River.
153. Magnetic ore from one foot layer, East Boulder Plateau.
154. Disseminated chromite, Gish property, Boulder River area.
155. Magnetic ore from West Fork of Stillwater River.
156. Chromite ore from Line Creek Plateau, Carbon County, Montana. Collected by A. L. Howland, 1941.

157–177. Cuban ore. Collected by T. P. Thayer.
157. La Victoria mine, Oriente.
158. La Tibera mine, Oriente.
159. Amores mine, Tunnel No. 7, Oriente.
160. Amores mine, Tunnel No. 8, Oriente.
161. Potosi mine, Oriente.
162. Estrella de Mayari, Oriente.
163. Loma Alta mine, Oriente.
164. Bad Luck mine, Holguin.
165. Narciso mine, Punta Gorda.
166. S. orebody Cayoguan mine, Punta Gorda.
167. W. orebody Cayoguan mine, Punta Gorda.
168. Ofelia mine, Camaguey.
169. Aventura mine, Camaguey, at contact.
170. Aventura mine, Camaguey, 15 ft. from contact.
171. Aventura mine, Camaguey, 20 ft. from contact.
172. Aventura mine, Camaguey, 25 ft. from contact.
173. Aventura mine, Camaguey, 30 ft. from contact.
174. Aventura mine, Camaguey, 35 ft. from contact.
175. Aventura mine, Camaguey, 40 ft. from contact.
176. Lolita mine, Camaguey.
177. Jose mine, Camaguey.

178. Zumpang, Mexico. Collected by W. D. Johnston, Jr.

179–180. Jalapa, Guatemala. Collected by W. D. Johnston, Jr.
179. Salvador mine.
180. Esperanza Hill.

181. Float ore, Medallin, Colombia. Collected by W. D. Johnston, Jr.

182–192. Chromite ore from Brazil. Collected by W. D. Johnston, Jr.
182. Second class ore, Cascabulhos mine, Baia, Brazil.
183. Banded ore, Campinhos mine, Baia, Brazil.
184. Best ore, Coitezeiro.
185. Limero.
186. First class ore, Brezo del Salto.
187. Boa Vista, Saude.
188. Ore from No. 1 pit, Santa Luzia, Baia, Brazil.
189. Gray ore, Piûi, Minas Geraes, Brazil.
190. Coarse chromite crystals, Piûi, Minas Geraes.
191. Fine-grained black chromite, Piûi, Minas Geraes, Brazil.
192. Slickensided chromite, Piûi, Minas Geraes, Brazil.

193. Chromite concentrates from residual deposit, Ivy Creek, near Democrat, North Carolina. Collected by C. S. Ross, 1941.

194. Coarse massive chromite, Thetford, Quebec. Collected by W. E. Richmond.
195. Fine massive chromite, Thetford, Quebec. Collected by W. E. Richmond.

TABLE 2. ANALYSES

Sample No.	Concentrate				Crude Ore	
	Cr	Fe	Ratio Cr/Fe	Cr_2O_3	Cr_2O_3	% Chromite
53	36.54	11.54	3.17	53.39	48.52	91
54	37.1	12.8	2.90	54.2	35.8	66
55	38.0	12.4	3.06	55.5	39.8	72
56	38.3	12.1	3.16	56.0	40.0	71
57	38.5	10.9	3.53	56.2	36.5	65
58	38.1	11.9	3.20	55.6	37.5	68
59	37.6	9.7	3.87	54.9	43.8	80
60	38.9	9.8	3.97	56.8	31.9	55
61	38.3	14.6	2.62	56.0	12.4	22
62	39.4	11.4	3.46	57.6	47.6	83
63	40.3	12.1	3.33	58.8	46.4	79
64	39.7	12.8	3.10	58.0	21.5	37
65	40.1	11.0	3.64	58.6	25.6	44
66	40.7	10.0	4.07	59.4	40.0	67
67	40.4	12.1	3.34	59.0	32.3	55
68	39.5	14.7	2.69	57.7	13.7	24
69	39.6	13.7	2.89	57.9	21.9	38
70	16.8	17.7	.95	24.5	20.7	85
71	17.0	15.9	1.07	24.8	13.1	53
72	40.5	11.2	3.62	59.2	44.3	75
73	40.2	11.1	3.62	58.8	36.3	62
74	40.0	12.1	3.30	58.4	45.7	78
75	39.0	13.6	2.87	57.0	33.5	59
76	40.7	12.3	3.31	59.4	34.5	58
77	40.9	11.7	3.49	59.7	43.7	73
78	40.0	12.8	3.12	58.4	45.0	77
79	39.8	14.2	2.80	58.2	27.3	47
80	40.0	15.3	2.61	58.4	24.4	42
81	40.1	13.1	3.06	58.6	39.7	68
82	38.5	12.7	3.03	56.3	47.3	84
83	39.5	11.6	3.40	57.7	47.1	82
84	40.2	11.5	3.50	58.8	51.0	87
85	39.5	11.6	3.40	57.7	51.2	89
86	39.8	11.5	3.46	58.2	52.1	90
87	40.3	13.1	3.08	58.9	30.0	51
88	37.6	14.1	2.67	55.0	27.5	50
89	39.4	13.4	2.94	57.6	19.2	33
90	37.9	16.2	2.34	55.4	23.9	43
91	38.9	12.5	3.11	56.9	44.9	79
92	40.3	11.6	3.47	58.8	50.2	85
93	40.1	11.4	3.52	58.6	50.6	86
94	40.4	12.8	3.15	58.5	35.8	61

TABLE 2—*Continued*

Sample No.	Concentrate				Crude Ore	
	Cr	Fe	Ratio Cr/Fe	Cr_2O_3	Cr_2O_3	% Chromite
95	39.30	18.05	2.18	57.44	50.56	88
96	36.97	18.67	1.98	54.01	46.30	86
97	33.05	23.51	1.41	48.29	43.10	89
98	36.00	20.28	1.78	52.59	47.66	91
99	23.50	33.58	.70	34.32	20.08	59
100	33.47	28.51	1.17	48.90	25.45	52
101	36.48	20.87	1.75	53.30	34.80	65
102	38.27	18.88	2.03	55.91	46.38	83
103	37.02	22.12	1.67	54.12	18.65	34
104	35.96	16.66	2.16	52.55	40.13	76
105	33.40	23.17	1.44	48.80	25.48	52
106	35.70	18.48	1.93	52.19	29.09	56
107	38.82	13.41	2.90	56.75	46.18	81
108	41.4	13.5	3.07	60.4	52.8	87
109	40.3	13.0	3.10	54.2	51.7	88
110	37.1	15.8	2.35	58.2	56.4	97
111	34.6	12.0	2.88	50.5	44.4	88
112	37.85	18.61	2.03	55.29	4.88	9
113	38.89	14.49	2.68	56.80	32.37	57
114	36.19	12.56	2.88	52.87	38.9	74
115	37.42	13.49	2.77	54.68	25.4	47
116	35.98	14.30	2.52	52.58	15.5	29
117	35.99	13.12	2.74	52.59	45.4	86
118	37.40	13.76	2.72	54.65	38.5	70
119	34.42	15.47	2.23	50.30	7.1	14
120	38.65	14.41	2.68	56.47	7.6	13
121	37.40	13.74	2.72	54.65	12.6	23
122	37.15	13.61	2.73	54.27	7.4	13
123	31.31	14.39	2.18	45.78	8.3	18
124	32.70	14.79	2.21	47.78	7.1	15
125	35.21	13.81	2.55	51.45	19.1	37
126	40.10	14.75	2.72	58.58	23.51	40
127	38.82	14.32	2.71	56.73	41.43	73
128	37.47	18.86	1.99	54.75	15.42	28
129	37.08	20.52	1.81	54.18	9.13	17
130	37.01	14.13	2.62	54.07	44.1	82
131	35.80	17.39	2.06	52.32	23.5	45
132	4.57	62.28	.07	6.67	1.7	25
133	37.17	18.31	2.03	54.30	16.6	31
134	37.27	12.65	2.94	54.45	22.8	42
135	36.43	11.69	3.12	53.25	36.8	69
136	28.22	12.40	2.28	41.25	33.8	82

TABLE 2.—*Continued*

Sample No.	Concentrate				Crude Ore	
	Cr	Fe	Ratio Cr/Fe	Cr_2O_3	Cr_2O_3	% Chromite
137	41.08	13.00	3.16	60.00	40.85	68
138	29.21	11.62	2.52	42.70	30.50	71
139	28.10	13.51	2.08	41.03	14.50	35
140	39.43	16.36	2.41	57.62	30.70	53
141	32.09	17.22	1.86	46.78	41.73	89
142	32.18	18.93	1.70	47.00	41.60	89
143	32.67	18.29	1.79	47.71	40.18	84
144	28.78	21.21	1.36	42.03	11.76	28
145	31.72	19.46	1.63	46.37	34.40	74
146	30.71	19.25	1.60	44.89	37.67	84
147	30.70	19.09	1.61	44.83	32.60	73
148	29.32	18.12	1.62	42.85	24.57	57
149	31.00	17.38	1.78	45.29	41.84	92
150	31.62	14.36	2.20	46.21	37.32	81
151	30.05	17.63	1.70	43.90	41.00	93
152	31.48	19.37	1.62	45.99	36.88	80
153	32.23	16.95	1.90	47.10	41.42	88
154	27.72	19.47	1.42	40.51	13.38	33
155	31.06	16.75	1.85	45.39	35.07	77
156	34.02	19.26	1.77	49.71	34.25	69
157	38.00	11.37	3.34	55.54	48.49	87
158	25.91	10.26	2.53	37.88	25.78	68
159	24.1	12.06	1.99	35.3	30.19	86
160	26.4	11.10	2.37	38.4	33.50	87
161	27.3	14.35	1.90	39.9	37.90	95
162	38.96	11.00	3.54	56.91	47.02	83
163	38.70	11.30	3.42	56.57	53.84	95
164	26.40	11.96	2.21	38.46	25.40	66
165	26.41	10.00	2.64	38.59	37.55	97
166	26.92	9.72	2.77	39.35	38.32	97
167	26.29	9.73	2.70	38.40	37.56	98
168	24.31	11.73	2.07	35.52	26.90	76
169	24.03	9.88	2.43	35.13	31.93	91
170	23.43	10.34	2.27	34.25	27.83	81
171	24.32	10.00	2.43	35.55	30.91	87
172	25.65	9.95	2.58	37.49	30.70	82
173	24.32	9.86	2.47	35.54	32.05	90
174	24.13	10.53	2.29	35.28	31.07	88
175	24.30	10.40	2.34	35.50	32.75	92
176	24.50	10.77	2.28	35.80	34.44	96
177	24.31	11.32	2.15	35.51	30.79	87

TABLE 2—*Continued*

Sample No.	Concentrate				Crude Ore	
	Cr	Fe	Ratio Cr/Fe	Cr_2O_3	Cr_2O_3	% Chromite
178	31.70	15.02	2.11	46.32	35.32	76
179	40.63	11.91	3.41	59.39	52.18	88
180	41.63	10.51	3.96	60.82	58.50	96
181	32.72	10.19	3.21	47.81	36.98	77
182	38.39	14.69	2.61	56.09	46.73	83
183	38.70	15.23	2.54	56.58	30.86	55
184	38.46	12.51	3.07	56.20	47.80	85
185	33.49	24.72	1.35	48.93	28.39	58
186	37.58	13.58	2.77	54.90	47.40	86
187	34.92	12.59	2.77	51.03	36.82	72
188	35.33	12.61	2.80	51.64	40.80	79
189	33.19	17.55	1.89	48.50	42.30	87
190	36.98	14.53	2.55	54.02	53.58	99
191	35.70	12.95	2.76	52.18	50.97	98
192	35.40	13.71	2.58	51.76	48.08	93
193	37.82	—	—	55.25	—	—
194	38.29	13.03	2.94	55.95	30.69	87
195	37.03	17.88	2.07	54.13	30.18	81

IV. Summary of analyses

The outline map of the Western Hemisphere (Fig. 1) summarizes the results of the analyses in Tables 1 and 2. At each locality the number of analyses is first given, followed by the average ratio of chromium to iron in the chromite; for example, one sample from the northernmost locality shown in Fig. 1 had a chromium-to-iron ratio of 3.2, showing that the deposit may be of metallurgical grade and worthy of further study. In areas from which a large number of samples have been taken the average ratio of chromium to iron, given in Fig. 3, shows the approximate grade of the chromite mineral at that place.

ISOMORPHISM IN CHROMITE

I. Previous work, and purpose of study of isomorphism

The composition of chromite is expressed by the formula $(Mg,Fe)O \cdot (Cr,Al,Fe)_2O_3$. The analyses in Table 1 show that ferric oxide is generally present, frequently as a minor constituent and commonly as a major constituent.

Simpson[5] and later Winchell[6] calculated chromite to four end members, formed by combining a molecule of Cr_2O_3 or Al_2O_3 with one of FeO or MgO. Such a simplification, although convenient, does not give the composition of chromite precisely, as ferric oxide, apparently ever present, is not taken into account. Fisher[7] suggests the same end members, but adds to them magnesioferrite, $MgO \cdot Fe_2O_3$, to account for the content of ferric oxide.

The purpose of this section is to determine what limitations there are in the substitution of one ion for another in the chromite formula $(Mg,Fe)O \cdot (Cr,Al,Fe)_2O_3$, and, if such limitations of isomorphism are found, to divide the chromites into groups in accordance with these facts. A relatively simple system of four end members to include the Fe_2O_3 content is also described.

II. The spinel group

The spinel group includes those isometric minerals of composition $RO \cdot R_2O_3$. Generally several ions substitute for one another in the formula, so that a close approximation to simple formulas by the minerals is seldom found.

The simple end-member formulas, which probably occur in minerals to a considerable extent, are as follows:

Aluminum spinels	*Iron (Fe^{+++}) spinels*	*Chromium spinels*
$MgO \cdot Al_2O_3$, Spinel	$MgO \cdot Fe_2O_3$, Magnesioferrite	$MgO \cdot Cr_2O_3$, Magnesiochromite
$MnO \cdot Al_2O_3$, Galaxite	$MnO \cdot Fe_2O_3$, Jacobsite	—
$FeO \cdot Al_2O_3$, Hercynite	$FeO \cdot Fe_2O_3$, Magnetite	$FeO \cdot Cr_2O_3$, Ferrochromite
$ZnO \cdot Al_2O_3$, Gahnite	$ZnO \cdot Fe_2O_3$, Franklinite	—
	$NiO \cdot Fe_2O_3$, Trevorite	—

Most of the spinels are isomorphous mixtures of several end members. Out of these eleven named members of the spinel group, only a few (spinel, $MgO \cdot Al_2O_3$; magnetite, $FeO \cdot Fe_2O_3$; and trevorite, $NiO \cdot Fe_2O_3$) are found with a composition within 90 per cent of the formula given.

Chromites have a wide range in composition as the result of the substitution of magnesia for ferrous iron and of aluminum and ferric iron for chromium. The analyses here given indicate that terrestrial chromites are predominantly $MgO \cdot Cr_2O_3$; for this reason $FeO \cdot Cr_2O_3$ is not considered the ideal formula for chromite and this end member is called ferrochromite in the above list of end members.

---

[5] Simpson, E. S., A graphic method for the comparison of minerals with four variable components forming two isomorphous pairs: *Mineral. Mag.*, **19**, 99 (1920).

[6] Winchell, A. N., The spinel group: *Am. Mineral.*, **26**, 422 (1941).

[7] Fisher, Lloyd W., Chromite: its mineral and chemical composition: *Am. Mineral.*, **14**, 341 (1929).

III. Variation in the size of the unit cell of chromites of different compositions

Great advances in the understanding of atomic arrangement in crystals have resulted in recent years through studies by means of x-rays. The unit-cell size of a number of the analyzed chromites of the present study was determined by W. E. Richmond by x-ray powder pictures. In addition Richmond determined the unit-cell size of two specimens that had been described by Simpson: one is spinel containing no chromium,[8] the other containing 22.76 per cent Cr_2O_3.[9] Although these two samples were not the original powder analyzed, the x-rayed samples were chips furnished by Dr. Simpson from the original specimen.

TABLE 3. VARIATION OF UNIT CELL-EDGE LENGTH WITH CHROMIUM CONTENT
(X-ray measurements by W. E. Richmond)

Sample No.	a_ω	% Cr_2O_3
S_1	8.103	0.0
S_2	8.175	22.76
70	8.190	24.5
1	8.273	31.31
24	8.213	32.2
2	8.250	34.81
25	8.224	35.5
123	8.257	45.75
12	8.248	47.57
124	8.256	47.78
5	8.267	48.45
4	8.263	48.55
125	8.270	51.45
117	8.270	52.59
6	8.277	52.77
114	8.270	52.87
135	8.284	53.25
122	8.282	54.27
121	8.285	54.65
118	8.281	54.65
88	8.288	55.0
120	8.290	56.47
3	8.292	57.83
76	8.305	59.4
18	8.295	59.40
66	8.301	59.4
76	8.301	59.5

---

[8] Simpson, Edward S., Famous mineral localities: Wodgina, North West Australia: *Am. Mineral.*, **13,** 461 (1928).

[9] Simpson, Edward S., A graphic method for the comparison of minerals with four variable components forming two isomorphous pairs: *Mineral. Mag.*, **19,** 99 (1920).

Richmond's results for the cell-edge length of the samples measured are given in Table 3, the two samples furnished by Dr. Simpson being listed as S_1 and S_2 at the head of the table. The cell-edge length (a_ω) of spinel, containing little chromium or ferric iron, is small (8.103Å units). With increase in chromium content the cell-edge length increases to more than 8.3Å units while increase of ferric iron content increases the size still more (the unit cell length of magnetite $FeO \cdot Fe_2O_3$ being about 8.4Å units). Interchange of ferrous iron and magnesia apparently have only a minor effect on the cell size.

Richmond's results for the cell-edge lengths are plotted against the chromium content in Fig. 2. The results fall roughly on a straight line, except where the ferric iron content is appreciable as in samples 1 and 2.

In most of the samples in which complete analyses were made, ferric oxide is present as a minor constituent in the R_2O_3 group and in these magnesia predominates over ferrous oxide in the RO group. As the proportion of ferric oxide increases, ferrous oxide also, in general, becomes greater, finally approaching the composition of magnetite, $FeO \cdot Fe_2O_3$.

Of the *x*-ray pictures taken only one high in iron showed double lines indicating the presence of magnetite as an impurity in the sample. Whenever possible magnetite had been removed with a magnet but in samples high in iron the chromite itself was highly magnetic making such a separation impracticable.

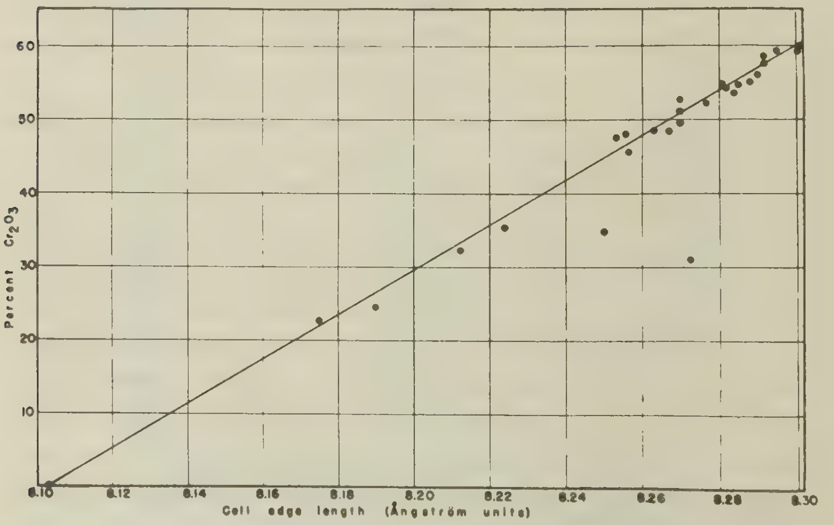

FIG. 2. Unit cell-edge length and Cr_2O_3 content of some chromites.

IV. Calculation of the ionic content of chromite unit cells from the analyses

According to Bragg[10] unit cells of the spinel structure contain $8(RO \cdot R_2O_3)$. Assuming this unit-cell content, the number of atoms of each metal present in the unit cell was calculated from the analyses in Table 2.

The calculations were made as follows: molecular ratios of the oxides were first obtained by dividing the percentage of each oxide by its molecular weight. The ratio of RO to R_2O_3 was then calculated after subtracting ilmenite and the silicate impurity. In samples having a ratio of RO to R_2O_3 appreciably less than 1, oxidation of ferrous to ferric oxide was assumed, and the analyses were recalculated to agree with the spinel formula. The molecular ratios were then recalculated to atoms per unit cell, assuming 8 bivalent and 16 trivalent metal ions as given by Bragg.

For example the calculation of atoms per unit cell for sample 37 is as follows:

	%	*Molecular Wt.*	*Molecular ratios*		*atoms/unit cell*	
Cr_2O_3	44.44	152.02	.2922		Cr	9.08
Al_2O_3	18.60	101.94	.1825		Al	5.66
Fe_2O_3	6.53	159.68	.0409		Fe^{+++}	1.26
			.5156			16.00
FeO	18.01	71.84	.2509	$-.0059^a = .2450$	Fe^{++}	3.78
MgO	11.16	40.32	.2769		Mg	4.22
MnO	.18	70.93	.0025			—
CaO	.02	56.08	.0004			—
			.5307	$-.0119^b = .5188$		8.00
TiO_2	.47	79.90	.0059			
SiO_2	.18	60.06	.0030			
	RO/R_2O_3	$\frac{.5188}{.5156} = 1.01$				

[a] Subtracting .0059 for ilmenite.

[b] Subtracting .0059 for ilmenite and .0060 for olivine.

The number of atoms of the different metals per unit cell, calculated from the analyses in Table 1, are given in Table 4, in order of increasing content of ferric iron. The samples marked with an *x* are those in which the determined FeO gave an RO to R_2O_3 ratio less than .95, and they have been recalculated to agree with the spinel formula. Those marked *o* are samples in which FeO was not determined, whereas samples unmarked are those in which the ratio of RO to R_2O_3 was 1 within experimental error (.95 to 1.05).

---

[10] Bragg, W. L., *Atomic Structure of Minerals*, p. 98, Cornell University Press, Ithaca, N. Y. (1937).

Table 4. Atoms per Unit Cell in Order of Increasing Ferric Iron

Unit cell content taken as 8(RO·R_2O_3)
Total $R^{+++}=16$, Total $R^{++}=8$

Sample No.	Cr	Al	Fe^{+++}	Fe^{++}	Mg
43 *x*	3.99	11.90	.11	2.40	5.60
42	11.56	4.18	.26	2.74	5.26
46 *o*	11.38	4.19	.43	2.62	5.38
48 *x*	11.68	3.86	.48	3.16	4.84
39	6.54	8.93	.51	2.24	5.76
41	7.90	7.52	.58	2.27	5.73
51 *x*	9.76	5.66	.58	2.66	5.34
10 *x*	11.50	3.91	.59	2.89	5.11
19	12.35	3.04	.61	2.98	5.02
47	8.10	7.30	.62	2.37	5.63
18	12.20	3.15	.66	3.06	4.94
40	6.78	8.54	.67	2.39	5.61
11	10.39	4.93	.69	3.06	4.94
23	7.12	8.19	.69	2.47	5.53
49	11.87	3.44	.69	2.92	5.08
36	9.38	5.89	.75	3.91	4.09
44 *o*	12.51	2.75	75	2.66	5.34
3	12.10	3.09	.82	3.24	4.76
45 *o*	12.58	2.58	.83	2.28	5.72
15 *o*	12.19	2.91	.90	3.06	4.94
50	11.75	3.33	.91	2.66	5.34
12	9.52	5.57	.91	2.82	5.18
13	11.70	3.38	.93	2.46	5.54
16 *o*	11.50	3.57	.93	3.34	4.66
9	11.50	3.55	.94	4.56	3.44
34 *o*	9.27	5.80	.96	3.92	4.08
22	6.85	8.16	.99	2.66	5.34
24	6.05	8.96	.99	2.45	5.55
17 *o*	12.04	2.93	1.04	3.79	4.21
21 *o*	11.49	3.49	1.04	3.37	4.63
38	9.79	5.17	1.04	3.53	4.47
20 *o*	11.68	3.27	1.06	3.46	4.54
14	11.75	3.06	1.20	2.86	5.14
7	11.47	3.31	1.22	2.74	5.26
33 *c*	9.07	5.66	1.26	4.37	3.63
37	9.08	5.66	1.26	3.78	4.22
52	10.72	4.00	1.30	2.49	5.51
6 *x*	11.33	3.30	1.38	3.47	4.53
5	10.11	4.50	1.39	3.78	4.22
4	9.82	4.78	1.41	3.42	4.58
31	9.16	5.41	1.42	3.86	4.14
25	6.93	7.60	1.47	2.49	5.51
35	9.32	5.22	1.49	3.66	4.34

TABLE 4—*Continued*

Unit cell content taken as $8(RO \cdot R_2O_3)$ Total $R^{+++}=16$, Total $R^{++}=8$					
Sample No.	Cr	Al	Fe^{+++}	Fe^{++}	Mg
8	11.78	2.58	1.65	3.34	4.66
32 *o*	9.54	4.80	1.66	3.49	4.51
2	7.02	6.91	2.08	4.34	3.66
27 *x*	9.62	3.39	3.01	6.26	1.74
1	6.82	5.40	3.79	4.99	3.01
30 *x*	8.32	.90	6.80	7.01	.99
26 *x*	6.45	1.78	7.80	7.38	.62
29 *x*	4.82	1.12	10.08	7.67	.33
28 *x*	3.28	1.20	11.52	7.44	.56

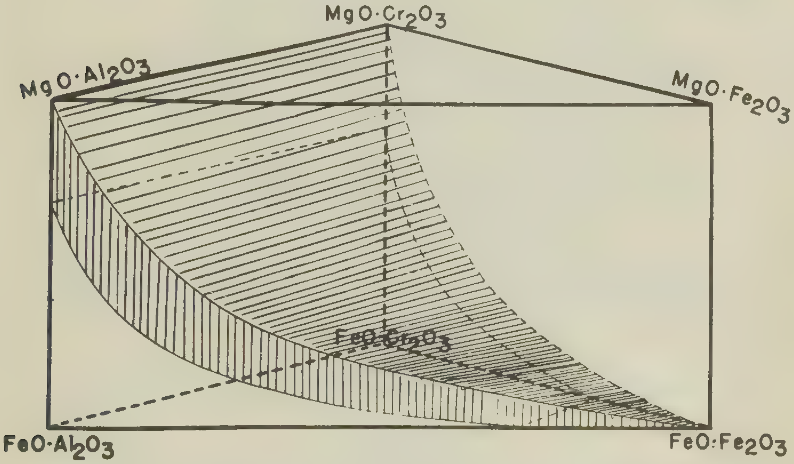

FIG. 3. The spinel triangular prism of composition, showing predominant zone of isomorphism.

V. The spinel triangular prism of composition

Variations in the content of the three trivalent ions in the unit cell may be represented on a triangular diagram such as that shown in Fig. 5. If the variations in the two bivalent ions are represented perpendicular to this triangle, a triangular prism results, as shown in Fig. 3. The six end members lie at the corners of the solid figure. Thus, assigning the ferrous iron to the base of the figure, the resulting end members are: ferrochromite, $FeO \cdot Cr_2O_3$; hercynite, $FeO \cdot Al_2O_3$; and magnetite, F_eO

$\cdot Fe_2O_3$. Magnesium increasing as the top of the solid is approached, the end members at the top three corners are: magnesiochromite, $MgO \cdot Cr_2O_3$; spinel, $MgO \cdot Al_2O_3$; and magnesioferrite, $MgO \cdot Fe_2O_3$.

The number of variables in the composition of chromites requires a solid figure to represent them and, because the compositions are represented by points in the solid, the pattern of points will vary with the line of sight through the solid. If the triangular prism is viewed from the side with the aluminum and ferric iron end members superposed, the composition points seem widely scattered with the ferrochromite corner vacant. As seen sidewise with the chromium and ferric iron end members in superposition, the half of the figure containing the end member hercynite is essentially not represented by any of the samples.

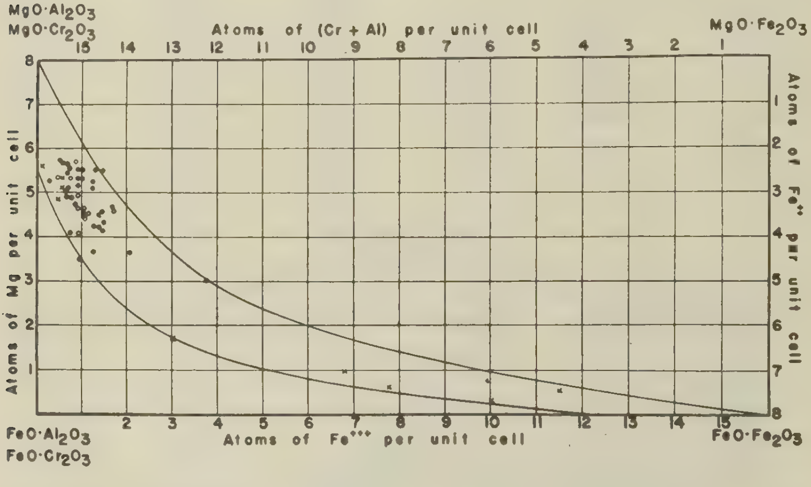

FIG. 4. View through spinel triangular prism with line of sight parallel to lines of equal Fe^{+++} content.

° FeO calculated.
× $RO/R_2O_3<1$
• $RO/R_2O_3=1$

The view of the spinel triangular prism of composition which best shows the trend of isomorphism in the chromites analyzed is that in Fig. 4, looking parallel to the lines of equal ferric iron content, with the aluminum and chromium end-members superposed. In this view a curved zone of isomorphism is apparent, corresponding to the shaded space in Fig. 3.

VI. Composition types in chromium-bearing spinel minerals

Figure 4 shows the apparent zone of isomorphism in the analyzed chromites. This zone extends from magnetite (lower right in Fig. 4) to spinel and magnesiochromite (top left), the zone bending somewhat toward the ferrochromite and hercynite end members. That the compositions of most chromites will be within this zone seems probable because of the large number of samples represented and their wide distribution. By means of this relationship the content of ferrous iron may be estimated from the composition of the trivalent ions, and, applying this relationship to the triangular diagram, simple division of chromium-bearing spinels results.

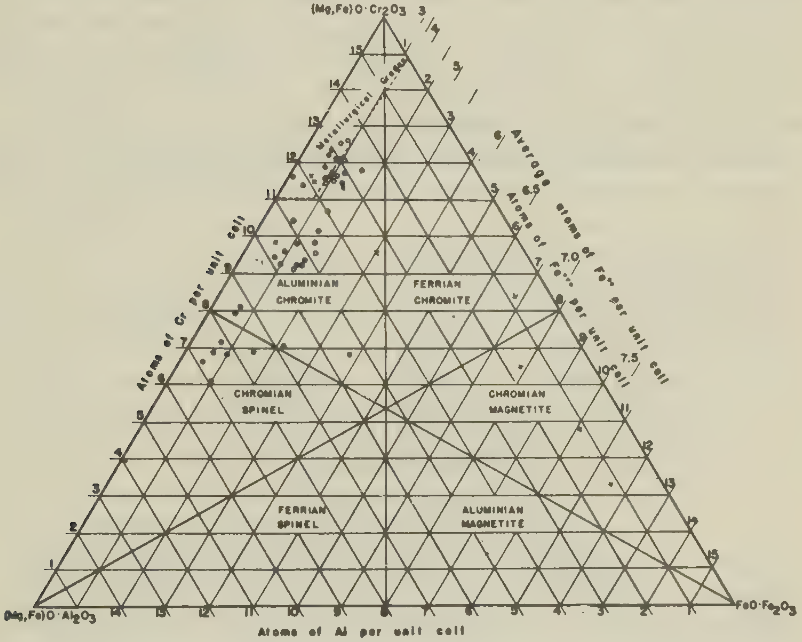

FIG. 5. Triangular diagram showing compositions of chromites and related minerals of the spinel group.

° FeO calculated.
× $RO/R_2O_3<1$
• $RO/R_2O_3=1$

The triangular diagram, Fig. 5, may be divided into areas representing six composition types by running diagonals from the corners containing the end members, to the center of the opposite side. Spinels falling in the upper two segments, in which Cr_2O_3 is the major constituent in the R_2O_3 group, may be classified as chromite; those falling in the lower left two segments, in which Al_2O_3 predominates, may be classified as spinel; and those in the lower right segments, with Fe_2O_3 predominating, may be classified as magnetite. Further division arises from the fact that in each of the six segments in Fig. 5 one of the minor constituents in the R_2O_3 group is in excess of the other. Ferrous as well as ferric iron increases toward the magnetite side until finally the composition of the magnetite end member, $FeO \cdot Fe_2O_3$, is attained.

Chromium-bearing spinels may therefore be classified according to composition as follows:

I. Chromite: $(\overrightarrow{\text{Mg, Fe}})\text{O} \cdot (\text{Cr}, \overleftrightarrow{\text{Al, Fe}})_2\text{O}_3$.
  A. Aluminian chromite: $(\overrightarrow{\text{Mg, Fe}})\text{O} \cdot (\text{Cr, Al, Fe})_2\text{O}_3$.
  B. Ferrian chromite: $(\overrightarrow{\text{Mg, Fe}})\text{O} \cdot (\text{Cr, Fe, Al})_2\text{O}_3$.
II Magnetite: $(\text{Fe, Mg})\text{O} \cdot (\text{Fe}, \overleftrightarrow{\text{Cr, Al}})_2\text{O}_3$.
  A. Chromian magnetite: $(\text{Fe, Mg})\text{O} \cdot (\text{Fe, Cr, Al})_2\text{O}_3$.
  B. Aluminian magnetite: $(\text{Fe, Mg})\text{O} \cdot (\text{Fe, Al, Cr})_2\text{O}_3$.
III. Spinel: $(\overrightarrow{\text{Mg, Fe}})\text{O} \cdot (\text{Al}, \overleftrightarrow{\text{Cr, Fe}})_2\text{O}_3$.
  A. Chromian spinel: $(\overrightarrow{\text{Mg, Fe}})\text{O} \cdot (\text{Al, Cr, Fe})_2\text{O}_3$.
  B. Ferrian spinel: $(\overrightarrow{\text{Mg, Fe}})\text{O} \cdot (\text{Al, Fe, Cr})_2\text{O}_3$.

In these formulas the elements in each group are written in order of abundance. The double arrow ($\leftrightarrow$) indicates that either of two elements may exceed the other; the single arrow ($\rightarrow$) that the first written element normally is in excess of the other.

In naming the sections a system of descriptive names has been used rather than assigning distinct mineral names to different parts of the diagram. This has been done for two reasons. First, the descriptive names are self-explanatory. The name picotite, for example, has not been used to refer to an intermediate composition because it is neither self-explanatory nor necessary. Secondly, the assignment of distinct mineral names to the sections implies distinct intermediate compositions approximated closely by many analyses, while the actual analyses indicate complete isomorphism within the zone.

Most metallurgical grades of chromite are within the area outlined with dashed lines at the top of Fig. 5. Here a low content of both ferrous and ferric iron, and a high chromium content result in a chromium-iron ratio of at least 3 to 1. As the content of ferrous iron is only approximately given in Fig. 5 the area of metallurgical grades cannot be exactly outlined.

Presumably none of the analyses quoted in this paper are of ferrian spinel and aluminian magnetite, because the present study concerns only high-chromium materials. Analyses of low-chromium spinels may be found in the literature. Although ferrian chromite is represented by only one of the complete analyses, some of the partial analyses are probably of ferrian chromites. Ferrian chromite is characterized by both a high chromium and a high total iron content and partial analyses having this character are those of samples 61, 80, 90, 95, 100, 105, 110, 112, and others.

VII. Expression of analyses in terms of end-members

At times expression of analyses as percentages of end-member spinels may be convenient, though admittedly an arbitrary mode of expression, and a suggested method of expressing results in terms of end members will accordingly be described.

The apices of the triangular prism of composition shown in Fig. 3 represent six end members, only four of which are needed to define any given composition within the solid. However, an arbitrary choice must be made of the four end members to be used since as many as four different end-member expressions may be used to represent a composition within the solid. For example, sample 42 may be expressed by the following four end-member systems:

1. spinel, magnesiochromite, ferrochromite, and magnetite;
2. hercynite, magnesiochromite, ferrochromite, and magnetite;
3. magnesioferrite, magnesiochromite, ferrochromite, and spinel;
4. hercynite, magnesioferrite, magnesiochromite, and ferrochromite.

The end-member system that suffices to express all but four of the 52 complete analyses, and all of those classified as chromite in the foregoing section, is the first of the end-member systems listed above; namely, spinel, magnesiochromite, ferrochromite, and magnetite.

End-member formulas per unit cell are calculated by the following equations:

$$\text{Spinel} = \frac{\text{Al}}{2}$$

$$\text{Magnesiochromite} = \text{Mg} - \frac{\text{Al}}{2}$$

$$\text{Ferrochromite} = \frac{\text{Cr}+\text{Al}}{2} - \text{Mg}$$

$$\text{Magnetite} = \text{Fe}^{++} + \text{Mg} - \frac{\text{Cr}+\text{Al}}{2} = \frac{\text{Fe}^{+++}}{2},$$

where each of the elements is given in atoms per unit cell.

To calculate the weight percentages of end members the formulas per unit cell are merely multiplied by the molecular weights of the end members and recalculated to 100 per cent.

As an example, sample 42, calculated to end members from the atoms per unit cell given in Table 3, gives the following figures:

	Formulas/unit cell	Formulas×M.W./unit cell	Wt%
spinel	2.09	297	19.5
magnesiochromite	3.17	610	40.1
ferrochromite	2.61	584	38.4
magnetite	.13	30	2.0

Formulas per unit cell may be converted to formula percentages by multiplying by 100 and dividing by 8.00.

A report of the other analyses in terms of end members does not seem to serve any useful purpose at the present time.

Acknowledgments

Grateful acknowledgment is made of the help of a number of persons both within and outside of the Geological Survey who have contributed much to this report.

Many of the purifications and partial analyses of chromite were made by M. K. Carron of the Geological Survey.

The triangular prism of composition used to explain the compositions of chromites was the conception of W. D. Johnston, Jr., of the Survey.

The interest and advice of W. D. Johnston, Jr., J. W. Peoples, F. G. Wells, and T. P. Thayer during the work and in the writing of the report was of great value. These and other geologists have submitted the samples, the analyses of which constitute this report. Sampling of the Kenai Peninsula, Alaska, chromite deposit is the work of P. W. Guild of the Survey.

The investigation was done under the direction of R. C. Wells, Chief Chemist of the Geological Survey, whose advice was of value throughout the investigation.

Review and criticism of the manuscript by H. G. Ferguson, W. T. Schaller, and Michael Fleischer, of the Survey led to many improvements.

Valuable information on methods of analysis of chrome ores was obtained in discussions with W. J. Boyer of the Rustless Iron and Steel Corporation, Baltimore, Md., and with Gilbert E. Seil, Technical Director of E. J. Lavino and Company, Plymouth Meeting, Pa.

The methods of heavy-solution mineral separations of L. H. Bauer of the New Jersey Zinc Co., Franklin, N. J., were adopted in the latter part of this investigation, and no doubt will be found useful in studying other minerals as well. Dr. Bauer gave liberally of his time in explaining and demonstrating these methods to the writer.

CRYSTALLOGRAPHY OF CALCITE FROM LAKE SUPERIOR COPPER MINES

CHARLES PALACHE,
*Harvard University, Cambridge, Massachusetts**

In 1898 the writer published a paper (Palache, 1898) on the crystallography of Lake Superior calcite. Although a large number of new calcite forms were described and illustrated in this paper, the measurements upon which they were based were omitted; the statement made there (page 183) that the observational data for the new forms would appear shortly in the *Zeitschrift für Krystallographie* was never justified by fulfillment of the promise. However, twenty-four of the thirty-two forms then proposed were included in the *Winkeltabellen* of V. Goldschmidt (1897), with calculated position angles, much of the study having been conducted in his laboratory. The figures were all reproduced in the same author's *Atlas der Krystallformen*, Vol. II, Plates 112–114, figures 1887–1910.

The author can offer no adequate excuse for this failure to publish his observations save the fact that the study continued from year to year as new and often very interesting material came into his hands. The summer of 1906 was partly spent on the Copper Range, examining the local collections and collecting material for an intended study of the local mineralogy, which was never completed. Again in 1920 and 1921 the author worked with the group of geologists who gathered the materials for *U. S. G. S. Professional Paper* **144** on the copper deposits and thus collected at first hand a great variety of calcite crystals. A paper containing all the results and elaborate zonal discussion of the forms was prepared but for forgotten reasons was never sent to press.

This paper is now presented in abbreviated form after a review of the older results and an examination of new crystals. The paper of 1898 may still serve as giving an adequate general description of the occurrence of calcite in the Lake Superior region.

Table 1 contains a list of 138 forms found on the nearly 200 crystals measured—a number which may be compared with 87 forms found on the 150 crystals described in the first paper. This increase shows how enormously rich and varied in development these crystals really are. The last column of the table states the number of crystals on which each form was observed and may serve as sufficient description of their relative importance. Those forms preceded by an asterisk were new for calcite in 1898, or have since been discovered; they number thirty-two and are collected in Table 2 together with the observed angles, range, and calculated position angles. These forms vary in importance from a few which are characteristic for the region and have since been found elsewhere, to the other extreme of purely local development. They will be briefly described in the order of enumeration.

---

* Contribution from the Department of Mineralogy and Petrography, Harvard University, No. 260.

TABLE 1. FORMS FOUND ON LAKE SUPERIOR CALCITE

		Bravais	Miller	No. of. xls.			Bravais	Miller	No. of xls
1	*o*	0 0 0 1	1 1 1	57	78	*ϕ*.	0 2 $\bar{2}$ 1	1 1 $\bar{1}$	45
2	*a*	1 1 $\bar{2}$ 0	1 0 $\bar{1}$	11	80	*F*.	0.12.$\overline{12}$.5	17.17.$\overline{19}$	1
3	*b*	1 0 $\bar{1}$ 0	2 $\bar{1}$ $\bar{1}$	7	82	*ω*.	0.11.$\overline{11}$.4	5 5 $\bar{6}$	1
5	*θ*	2 1 $\bar{3}$ 0	5 $\bar{1}$ $\bar{4}$	3	83	Γ.	0 3 $\bar{3}$ 1	4 4 $\bar{5}$	1
6	*ζ*	3 1 $\bar{4}$ 0	7 $\bar{2}$ $\bar{5}$	2	86	Δ.	0 7 $\bar{7}$ 2	3 3 $\bar{4}$	3
8	*ψ*	10.1.$\overline{11}$.0	7 $\bar{3}$ $\bar{4}$	14	87	Θ.	0 4 $\bar{4}$ 1	5 5 $\bar{7}$	1
9	*π*	1 1 $\bar{2}$ 3	2 1 0	2	92	*Q*.	0 7 $\bar{7}$ 1	8.8.$\overline{13}$	1
11	λ	2 2 $\bar{4}$ 3	3 1 $\bar{1}$	2	93	Π.	0 8 $\bar{8}$ 1	3 3 $\bar{5}$	15
12	*ν*	1 1 $\bar{2}$ 1	4 1 $\bar{2}$	2	96	Σ.	0.11.$\overline{11}$.1	4 4 $\bar{7}$	1
13	*α*	4 4 $\bar{8}$ 3	5 1 $\bar{3}$	2	98	*C*.	0.13.$\overline{13}$.1	14.14.$\overline{25}$	1
14*	*ω*	16.16.$\overline{32}$.9	19.3.$\overline{13}$	5	99	Φ.	0.14.$\overline{14}$.1	5 5 $\bar{9}$	1
15	*ξ*	2 2 $\bar{4}$ 1	7 1 $\bar{5}$	$\bar{5}$	113	*W*:	13.11.$\overline{24}$.2	13.0.$\overline{11}$	1
17	*γ*	8.8.$\overline{16}$.3	9 1 $\bar{7}$	5	117	*U*:	5 4 $\bar{9}$ 1	5 0 $\bar{4}$	2
26	*p*.	1 0 $\bar{1}$ 1	1 0 0	121	119	*x*:	4.3.$\bar{7}$.10	7 3 0	3
28	*R*.	2 0 $\bar{2}$ 1	5 $\bar{1}$ $\bar{1}$	1	122	*T*:	4 3 $\bar{7}$ 1	4 0 $\bar{3}$	1
29	*K*.	5 0 $\bar{5}$ 2	4 $\bar{1}$ $\bar{1}$	6	125	*ζ*:	7.5.$\overline{12}$.2	7 0 $\bar{5}$	1
31	*m*.	4 0 $\bar{4}$ 1	3 $\bar{1}$ $\bar{1}$	128	129	*Q*:	19.13.$\overline{32}$.6	19.0.$\overline{13}$	1
40	*r*.	10.0.$\overline{10}$.1	7 $\bar{3}$ $\bar{3}$	7	133	*P*:	3 2 $\bar{5}$ 1	3 0 $\bar{2}$	11
43	*s*.	13.0.$\overline{13}$.1	9 $\bar{4}$ $\bar{4}$	1	135	*p*:	17.11.$\overline{28}$.6	17.0.$\overline{11}$	2
45	*v*.	18.0.$\overline{18}$.1	37.$\overline{17}$.$\overline{17}$	1	136*	*j*:	11.7.$\overline{18}$.4	11.0.$\bar{7}$	4
48	*z*.	28.0.$\overline{28}$.1	19.$\bar{9}$.$\bar{9}$	1	137		8.5.$\overline{13}$.6	9 1 $\bar{4}$	1
55	*δ*.	0 1 $\bar{1}$ 2	1 1 0	37	141	*N*:	5 3 $\bar{8}$ 2	5 0 $\bar{3}$	10
58	*η*.	0 4 $\bar{4}$ 5	3 3 $\bar{1}$	1	145	*v*:	7.4.$\overline{11}$.15	11.4.0	3
61	*θ*.	0 7 $\bar{7}$ 8	5 5 $\bar{2}$	1	146	𝔴:	7.4.$\overline{11}$.6	8 1 $\bar{3}$	6
64	λ.	0 8 $\bar{8}$ 7	5 5 $\bar{3}$	12	147	*M*:	7.4.$\overline{11}$.3	7 0 $\bar{4}$	5
65	*μ*.	0 6 $\bar{6}$ 5	11.11.7	3	425*	*q*:	9.5.$\overline{14}$.3	26.$\bar{1}$.$\overline{16}$	2
66	*ν*.	0 5 $\bar{5}$ 4	3 3 $\bar{2}$	3	151*	𝔟	20.11.$\overline{31}$.15	22.2.$\bar{9}$	5
67	*ξ*.	0 4 $\bar{4}$ 3	7 7 $\bar{5}$	8	153	*M*:	15.8.$\overline{23}$.10	16.1.$\bar{7}$	2
68	*π*.	0 7 $\bar{7}$ 5	4 4 $\bar{3}$	5	446		4 2 $\bar{6}$ 3	13.1.$\bar{5}$	1
70	*ρ*.	0 3 $\bar{3}$ 2	5 5 $\bar{4}$	7	155	𝔜:	19.10.$\overline{29}$.6	18.$\bar{1}$.$\overline{11}$	1
71	*σ*.	0.11.$\overline{11}$.7	6 6 $\bar{5}$	10	156*	𝔞	37.19.$\overline{56}$.21	38.1.$\overline{18}$	9
73	*τ*.	0.13.$\overline{13}$.8	7 7 $\bar{6}$	6	154	*L*:	17.9.$\overline{26}$.8	17.0.$\bar{9}$	1
75	*M*.	0 7 $\bar{7}$ 4	11.11.$\overline{10}$	1	158	𝔛	8.4.$\overline{12}$.7	9 1 $\bar{3}$	1

TABLE 1—*continued*

		Bravais	Miller	No. of xls			Bravais	Miller	No. of xls
159	ℨ	6 3 $\bar{9}$ 4	19.1.$\bar{8}$	3	238*	*x*	4.5.$\bar{9}$.14	9 5 0	4
160*	*M*	8.4.$\overline{12}$.5	25.1.$\overline{11}$	10	240*	*s*	16.20.$\overline{36}$.5	19.3.$\overline{17}$	5
161		12.6.$\overline{18}$.7	37.1.$\overline{17}$	2	243*	*t*	9.13.$\overline{22}$.5	12.3.$\overline{10}$	5
162	*K*:	2 1 $\bar{3}$ 1	2 0 $\bar{1}$	75	244	*y*:	2 3 $\bar{5}$ 8	5 3 0	2
165	𝔅:	16.8.$\overline{24}$.5	15.$\bar{1}$.$\bar{9}$	1	250*	*u*:	3.5.$\bar{8}$.13	8 5 0	9
453*	*r*:	32.14.$\overline{46}$.9	29.$\bar{3}$.$\overline{17}$	3	251	*b*:	3 5 $\bar{8}$ 4	5 2 $\bar{3}$	71
455*	*s*:	16.7.$\overline{23}$.1	40.8.$\overline{29}$	1	673?	*E*	32.56.$\overline{88}$.69	63.31.$\overline{25}$	1
180	*g*:	5 2 $\bar{7}$ 9	7 2 0	8	526*	*S*:	32.56.$\overline{88}$.45	55.23.$\overline{33}$	38
181	*J*:	5 2 $\bar{7}$ 3	5 0 $\bar{2}$	4	258	*C*	14.26.$\overline{40}$.21	25.11.$\overline{15}$	26
183*	*U*:	10.4.$\overline{14}$.3	9 $\bar{1}$ 5	31	263		7.14.$\overline{21}$.11	13.6.$\bar{8}$	Irby
189	*w*:	3 1 $\bar{4}$ 5	4 1 0	8	264	*E*:	5.10.$\overline{15}$.7	9 4 $\bar{6}$	3
190*	*N*	12.4.$\overline{16}$.11	13.$\bar{1}$.$\bar{3}$	14	265	𝔉:	4.8.$\overline{12}$.5	7 3 $\bar{5}$	7
191	*H*:	3 1 $\bar{4}$ 2	3 0 $\bar{1}$	27	268	𝔮:	2 4 $\bar{6}$ 1	3 1 $\bar{3}$	1
194	ℑ:	6 2 $\bar{8}$ 1	5 $\bar{1}$ $\bar{3}$	31	270	*F*	5.11.$\overline{16}$.6	9 4 7	4
196	*f*:	7.2.$\bar{9}$.11	9 2 0	6	544*	*I.*	17.38.$\overline{55}$.24	32.15.$\overline{23}$	3
197	*G*:	7 2 $\bar{9}$ 5	7 0 $\bar{2}$	1	549?	*A*	6.14.$\overline{20}$.7	11.5.$\bar{9}$	2
203	*e*:	4 1 $\bar{5}$ 6	5 1 0	2	274	*J*	8.20.$\overline{28}$.9	15.7.$\overline{13}$	10
204*	*Z*	16.4.$\overline{20}$.15	17.1.$\bar{3}$	13	276*	*D*	3.8.$\overline{11}$.4	6 3 $\bar{5}$	8
206	*F*:	4 1 $\bar{5}$ 3	4 0 $\bar{1}$	1	277	*Y*	12.32.$\overline{44}$.13	23.11.$\overline{21}$	19
211	𝔓:	5 1 $\bar{6}$ 1	4 $\bar{1}$ $\bar{2}$	11	282	𝔣𝔭:	1 3 $\bar{4}$ 1	2 1 $\bar{2}$	77
214	*D*:	6 1 $\bar{7}$ 5	6 0 $\bar{1}$	1	283		6.20.$\overline{26}$.13	15.9.$\overline{11}$	4
215	*A*:	24.4.$\overline{28}$.5	19.$\bar{5}$.$\bar{9}$	3	285*	*B*	12.40.$\overline{52}$.11	25.13.$\overline{27}$	4
217	*b*:	7 1 $\bar{8}$ 9	8 1 0	1	287	ℭ:	2 7 $\bar{9}$ 4	5 3 $\bar{4}$	1
219	Ξ:	14.2.$\overline{16}$.3	11.$\bar{3}$.$\bar{5}$	19	292	𝔤:	1 4 $\bar{5}$ 3	3 2 $\bar{2}$	2
220	*a*:	8.1.$\bar{9}$.10	9 1 0	2	293	*R*	8.32.$\overline{40}$.21	23.15.$\overline{17}$	1
221*	Λ:	32.4.$\overline{36}$.7	25.7.$\overline{11}$	15	296	𝔬:	2.8.$\overline{10}$.3	5 3 $\bar{5}$	1
222	*B*:	17.2.$\overline{19}$.15	17.0.$\bar{2}$	1	297	*Q*:	7.28.$\overline{35}$.9	17.10.$\overline{18}$	2
224*	Φ:	9.1.$\overline{10}$.2	7 $\bar{2}$ $\bar{3}$	5	298	𝔵:	4.16.$\overline{20}$.3	9.5.$\overline{11}$	15
501*	*t*:	37.4.$\overline{41}$.36	38.1.$\bar{3}$	1	299	𝔱	3.13.$\overline{16}$.8	9 6 7	8
226*	Π:	10.1.$\overline{11}$.3	8 $\bar{2}$ $\bar{3}$	12	301	𝔠	4.20.$\overline{24}$.17	15.11.$\bar{9}$	15
227*	Θ:	40.4.$\overline{44}$.9	31.$\bar{9}$.$\overline{13}$	14	303	𝔏:	2.10.$\overline{12}$.7	7 5 $\bar{5}$	1
229*	Σ:	22.2.$\overline{24}$.5	17.$\bar{5}$.7	7	304	𝔒:	4.20.$\overline{24}$.11	13.9.$\overline{11}$	3
231*	Δ:	13.1.$\overline{14}$.3	10.$\bar{3}$.$\bar{4}$	2	315	*D*:	2.13.$\overline{15}$.4	7 5 $\bar{8}$	1
503*	Ω:	32.2.$\overline{34}$.9	25.7.$\bar{9}$	1	319*	𝔡	4.36.$\overline{40}$.31	25.21.$\overline{15}$	6
232*	Γ:	17.1.$\overline{18}$.4	13.$\bar{4}$.$\bar{5}$	11	322*	*K*	1.11.$\overline{12}$.8	7 6 $\bar{5}$	4
233*	*y*	6 7 $\overline{13}$.20	13.7.0	3	300	𝔅:	2.9.$\overline{11}$.5	6 4 $\bar{5}$	1

The serial numbers used for each form in this table are taken from a recent paper by the author, Calcite, An Angle Table and Critical List, privately published in May, 1943, by the Dept. of Mineralogy and Petrography of Harvard University as Contribution No. 259. A limited number of copies of this paper are available at publication cost, 50 cents.

Numbers from 1 to 328 indicate the certain forms; from 329 to 630 the probable and uncertain forms; 631 to 696 the discarded forms.

* New forms.

TABLE 2. OBSERVED ANGLES OF NEW FORMS, LAKE SUPERIOR CALCITE

		Number		Range		Mean Value		Calculated Value	
		faces	xls.	ϕ	ρ	ϕ	ρ	ϕ	ρ
ω	$16.16.\overline{32}.9$	15	4	0°00′– 0°42′	71°35′–72°08′	0°06½′	71°47′	0°00′	71°46½′
j:	$11.7.\overline{18}.4$	5	3	7 10 – 7 24	75 14 –75 37	7 19	75 26	7 18½	75 32
q:	$9.5.\overline{14}.3$	3	2	9 26 – 9 28	76 05 –76 21	9 27	76 11	9 22	76 06
r:	$32.14.\overline{46}.9$	8	2	12 27 –12 53	77 17 –77 47	12 38½	77 33½	12 44	77 24½
s:	$16.7.\overline{23}.1$	4	1	12 34 –12 45	87 00 –87 05	12 41½	87 02½	12 44	87 09½
t:	$37.4.\overline{41}.36$	4	1	24 45 –25 10	46 58 –47 03	24 55½	47 01	24 55½	47 01
𝔟	$20.11.\overline{31}.15$	7	2	9 09 – 9 33	60 16 –60 47	9 21	60 31	9 31	60 49
𝔞	$37.19.\overline{56}.21$	14	5	10 43 –11 33	65 68 –66 59	11 10	66 23	10 31	66 39½
M	$8.4.\overline{12}.5$	26	9	10 30 –11 08	64 00 –64 44	10 48	64 20	10 53½	64 24½
U:	$10.4.\overline{14}.3$	35	10	13 43 –14 05	76 14 –76 28	13 54	76 19	13 54	76 19
N	$12.4.\overline{16}.11$	13	6	16 00 –16 13	52 16 –52 20	16 07	52 18½	16 06	52 17½
Z	$16.4.\overline{20}.15$	7	3	18 52 –19 25	50 19 –50 38	19 05½	50 25	19 06½	50 19½
Λ:	$32.4.\overline{36}.7$	12	7	24 00 –24 25	78 10 –78 24	24 12	78 18½	24 11	78 16
Φ:	$9.1.\overline{10}.2$	4	3	24 47 –24 58	78 00 –78 08	24 51½	78 05	24 47½	78 05
Π:	$10.1.\overline{11}.3$	21	9	24 35 –25 12	73 40 –73 58	24 53½	73 47	25 17	73 54
Θ:	$40.4.\overline{44}.9$	8	3	24 58 –25 27	77 42 -77 58	25 16	77 49½	25 17	77 47
Σ:	$22.2.\overline{24}.5$	12	7	25 22 –25 56	77 31 –77 48	25 39½	77 38½	25 41½	77 36½
Δ:	$13.1.\overline{14}.3$	4	2	26 14 –27 02	77 06 –77 22	26 33	77 16	26 20	77 20
Ω:	$32.2.\overline{34}.9$	2	1	26 49 –27 01	74 34 –74 34	26 55	74 34	26 59½	74 34
Γ:	$17.1.\overline{18}.4$	5	3	26 56 –27 19	76 57 –77 05	27 07½	77 00½	27 10	76 58
y	$6.7.\overline{13}.20$	7	4	1 57 – 3 04	28 59 –29 18	– 2 28	29 08	– 2 32½	29 04
x	$4.5.\overline{9}.14$	9	3	3 15 – 4 19	28 35 –29 09	– 3 53	28 49	– 3 40	28 49½
u:	$3.5.\overline{8}.13$	6	4	8 13 – 8 28	27 57 –28 06	– 8 20½	27 59	– 8 13	27 58½
s	$16.20.\overline{36}.5$	16	5	3 28 – 3 48	80 36 –80 50	– 3 40	80 43½	– 3 40	80 47
ι	$9.13.\overline{22}.5$	17	5	5 51 – 6 10	75 00 –75 28	– 5 59	75 10½	– 5 59½	75 11
E	$32.56.\overline{88}.69$	3	1	9 02 – 9 11	47 32 –47 58	– 9 07	47 42	– 8 57	47 48
S:	$32.56.\overline{88}.45$	30	17	8 33 – 9 06	59 13 –59 52	– 8 50	59 24½	– 8 57	59 24½
I·	$17.38.\overline{55}.24$	11	3	11 42 –12 22	63 07 –63 45	–12 04½	63 32	–12 26	63 29½
D	$3.8.\overline{11}.4$	21	8	14 20 –14 52	67 27 –67 41	–14 39	67 33½	–14 42½	67 37½
B	$12.40.\overline{52}.11$	4	2	17 12 –17 17	76 37 –76 43	–17 14	76 40	–17 16	76 42
𝔡	$4.36.\overline{40}.31$	12	6	24 35 –24 54	50 24 –50 34	–24 44	50 28½	–24 47½	50 31½
K	$1.11.\overline{12}.8$	19	4	25 21 –25 43	54 48 –54 58	–25 36	54 52½	–25 41½	54 53

ω$\{16.16.\overline{32}.9\}$—This dipyramid is well established by concordant measurements on a number of crystals. Its faces are of good quality and often of large size. It is illustrated in Fig. 9 of the 1898 paper and in Figs. 1 and 2 of this paper. It has been reported at Långban, Sweden, by Flink and Aminoff, and at French Creek, Pennsylvania, by Gordon.

j: $\{11.7.\overline{18}.4\}$—This scalenohedron of the principal zone is a minor form well established by the measurements shown in the table. It is not figured.

q⁝ $\{9.5.\overline{14}.3\}$, *r*⁝ $\{32.14.\overline{46}.9\}$, *s*⁝ $\{16.7.\overline{23}.1\}$, *t*⁝ $\{37.4.\overline{41}.36\}$.—These four new scalenohedrons were found on the crystal from the Tamarack Mine shown in Figs. 3 and 4. This unique crystal was loaned for study by the late Mr. Reeder of Houghton. It is a twin crystal of perfect symmetry and superb quality, its greatest dimension about one inch. The twin and contact plane is $(01\bar{1}2)$. The crystal was first measured with one individual in a normal position, and this is figured with approximate fidelity in Fig. 3. Besides the familiar Lake Superior forms, such as *p.*, *N*, *m.*, *U*⁝, *K:* and *Y*, there were found the new forms, developed in part as the largest and most brilliant faces on the crystal, each with two faces on each individual of the twin. *q*⁝ and *r*⁝ are particularly well developed and despite their large size gave single signals on the goniometer of great brilliance. So surprising was the presence of these new forms that they were measured four times with repeated readjustment of the somewhat unwieldy crystal, but the measurements were concordant. The table of angles shows that the forms give mean position angles in reasonably good agreement with the calculated values. There are no zonal relations which aid materially in establishing their symbols. The form $\{28.16.\overline{44}.9\}$ with phi 8°57′ and rho 76°41½′ is the known form nearest to *q*⁝. However, this form is in a zone determined by *m.* and *U*⁝, a zone in which the new form does not lie as may be seen in the drawing. *r*⁝ is close to the form $\{7.3.\overline{10}.2\}$ found by Flink at Långban but apparently not as well substantiated by Flink's measurements as is *r*⁝. In the fig. *K:* seems to symmetrically truncate the edge between *N* and *q*⁝ but in reality it is not quite in the zone. *t*⁝ is, on the other hand, in the zone determined by *p.* and *N;* but to make the symbol, complicated at best, conform to this zone prevents one from identifying it with either of the known forms near it in angle, all of which belong to the principal zone.

		ϕ	ρ
t⁝	$37.4.\overline{41}.36$	24°55½′	47°01′
A:	$11.1.\overline{12}.10$	25 41½	48 41
B:	$17.2.\overline{19}.15$	24 30	49 56½
	$10.1.\overline{11}.9$	25 17	49 06½

The four forms are put forward as highly probable, although not established by this one observation.

The crystal was also completely measured with the twin plane and the two basal planes vertical. The result is shown in Fig. 4, which is an orthographic projection normal to a face of $\{11\bar{2}0\}$. The figure is slighly idealized and some of the minor planes are omitted. No other crystal remotely like this one was seen among the many hundreds examined during this study.

𝔟$\{20.11.\overline{31}.15\}$, 𝔞$\{37.19.\overline{56}.21\}$—These two scalenohedrons are in a zone between *K*:$\{21\bar{3}1\}$ and $\pi\{11\bar{2}3\}$. They are weak forms but occur persistently, either together as shown on Fig. 6 (Palache, 1898) or each by itself as in Figs. 7 and 24. In the zone with them, well shown in Fig. 6, is another, more common Lake Superior form, 𝔴⁚ $\{7.4.\overline{11}.6\}$, first found by Irby and repeatedly in this study. *M*⁚ $\{15.8.\overline{23}.10\}$, found by Whitlock (1927) on New Jersey crystals and once on a Lake Superior crystal, is also in this zone.

M$\{8.4.\overline{12}.5\}$—This scalenohedron is an important member of the Lake Superior form series. It is shown in minor development in Fig. 9 (Palache, 1898). In Fig. 1 of this paper it is a major form and was seen on many crystals, always of good quality and in good position. It has been found also by Whitlock in New Jersey and by Gordon at French Creek, Pennsylvania.

U⁚ $\{10.4.\overline{14}.3\}$—This is the most important of the new forms. It was measured on ten crystals and seen on twenty others, always with faces of great perfection and in extremely accurate position. Its zonal position between *m*.$\{40\bar{4}1\}$ and $\gamma\{8.8.\overline{16}.3\}$ helps to identify it, as *m*. truncates it with parallel edges. It is shown in greater or less development in Figs. 2, 4, 5, 7, and 14 (Palache, 1898), indicated by the letter *U* without dots; in this paper it is shown in Figs. 3, 5, and 6. It was new in 1898 but has since been found at such widely separated localities as New York State (Whitlock, 1910); Långban (Aminoff, 1918); Terlingua, Texas (Eakle, 1907); Blaton, Belgium (Buttgenbach, 1920); and Lionsville, New South Wales (Smith, 1927). It takes rank as one of the common forms of calcite.

N$\{12.4.\overline{16}.11\}$—This is a strongly developed and rather common scalenohedron in Lake Superior crystals. Seen on fourteen crystals and measured on six, it shows a notable stability of position. It was figured on two combinations in 1898, Figs. 6 and 19. The relation of *N* to the group of negative scalenohedrons *b*⁚, *C* and *S*⁚ which are described later, is of special note. *N* has a strong tendency to form with *b*⁚ an oscillatory striation made up of brilliant facets parallel to the two forms. This stepped surface impinges upon *C* or *S*⁚, one of which forms is almost invariably present, in an irregular zig-zag intersection which cannot be accurately shown in a formal crystal drawing. Figure 7 is an attempt to show this relation, but the steps of the striation surface are too broad and too few to bring out the characteristic irregularity of the intersection with *C*. The relation is found repeatedly, often on large crystals of magnificent brilliancy and clearness. The zone *N–b*: contains a pole of *φ*.$\{02\bar{2}1\}$ and one of *Z*, next to be described. *N* and *Z* also form a simple zone with *p*. which contains $\{7.4.\overline{11}.6\}$, mentioned in a previous paragraph, and the important form $\{4.4.\bar{8}.3\}$. These zonal relations establish the importance of this new form, which has not as yet been found elsewhere.

Z$\{16.4.\overline{20}.15\}$—This scalenohedron was seen on as many as thirteen crystals but was measurable on only three. Its typical occurrence is on crystals of negative scalenohedral habit with narrow triangular facets as shown in Fig. 17 (Palache, 1898). But on Fig. 15 of the same plate the form *N* is shown with a similar appearance, and measurement is necessary to distinguish them. It is also shown with *N* in Fig. 6, and its zonal relation to that form has already been described.

The series of eight positive scalenohedrons beginning in Table 2 with the form Λ: $\{32.4.\overline{36}.7\}$ and ending with Γ: $\{17.1.\overline{18}.4\}$ were all reported in 1898, with the exception of the only doubtful one, Ω:. They form an interesting and very complex zone series lying on both sides of $\{40\bar{4}1\}$ in the direction of a face of the prism $\{11\bar{2}0\}$. Included with them in the zone are the much more important and common forms $\{14.2.\overline{16}.3\}$, $\{51\bar{6}1\}$, and $\{62\bar{8}1\}$, all of which, as shown in Table 1, are frequently occurring Lake Superior forms. The varied developments of this series on crystals of a variety of habits produce one of the most characteristic features of the calcite of this region. As may be seen from the angle table, they lie very near to each other, and therefore tend to produce a more or less striated surface when several are present. Even then, however, the signals from them are distinct, and each one of them has been observed at least once without another of the series. With the exception noted they are regarded as well established although but one of them, Φ: has as yet been found elsewhere. The series is shown in full development in Fig. 2 (Palache, 1898) and less fully developed in Figs. 5, 7, 14, and 19. Figures 3 and 5 of this paper also show some of these forms. Ω: $\{32.2.\overline{34}.9\}$ is shown in Fig. 5. Its position is good, but it is doubtful because not seen except on this one crystal.

y$\{6.7.\overline{13}.20\}$, *x*$\{4.5.\bar{9}.14\}$, and *u*:$\{3.5.\bar{8}.13\}$—These three negative scalenohedrons belong to that part of the crowded terminal principal zone of calcite lying between $\{01\bar{1}2\}$ and $\{11\bar{2}3\}$. The first two were found on several crystals of one specimen. The faces were distinct, present on each crystal in full number, and show little variation of position. They are shown in Fig. 8 in typical development. The third form, *u*:, was reported in 1898 and has a wider distribution, having been measured on four crystals and identified on several others. It is shown in Figs. 13 and 23 (Palache, 1898), in the latter truncating the edge between the base and *b*: {3.5.$\bar{8}$.4}. All three may be regarded as weak but well-established forms.

s{16.20.$\overline{36}$.5}, *t*{9.13.$\overline{22}$.5}—These two forms were found on the five measured crystals taken from a group from the Allouez Mine and were seen to be present on every crystal. They are generally small facets but in a few crystals are more largely developed. The reflections obtained from them were very good and the position angles show little variation, so the forms may be deemed established. They are shown in Fig. 6. Their zonal relations are not marked.

Probably more than half of the calcite crystals from Lake Superior Mines are dominated by negative scalenohedrons. This feature was stressed in the earlier report and many figures illustrate it. Figure 9 is introduced here to show the character of the simplest of these negative forms when symmetrically developed. The two forms *b*: {3.5.$\bar{8}$.4} and $\mathfrak{p}$: {13$\bar{4}$1} compose it and give character to many of the crystals. These two are also the most common negative scalenohedrons to be found on calcite the world over, but elsewhere they generally occur as minor modifying forms.

{13$\bar{4}$1} is a peculiarly stable form, faces measured on different crystals rarely varying more than a few minutes from the calculated position. This is not true of {35$\bar{8}$4}, however; when crystals bearing this form are measured, it is found that the position angles are variable through a considerable range of angle and often the faces are faceted and yield two or more sets of position angles. In other words, a vicinal development is common. In the following table are brought together the various forms found in the literature of calcite that group themselves about *b*:

			ϕ	ρ	
b:	$35\bar{8}4$	$52\bar{3}$	−8°13′	59°55′	Common
S:	$32.56.\overline{88}.45$	$55.23.\overline{33}$	−8 57	59 24½	New
C	$14.26.\overline{40}.21$	$25.11.\overline{15}$	−9 49½	58 48½	Irby (1)
	$29.51.\overline{80}.41$	$50.21.\overline{30}$	−9 0½	59 21½	Irby (2)
	$6.11.\overline{17}.9$	$32.14.\overline{19}$	−9 38½	58 34½	Irby (3)
	$56.98.\overline{154}.81$		−8 57	58 41½	Hessenberg (calculation in error due to false zone)
	$29.53.\overline{82}.43$	$154.\overline{67}.92$	−9 35	58 49	Cesàro (1891)

After studying the measurements of scores of crystals it was finally concluded that the existence of two vicinals to *b*: must be recognized: *C*, established by Irby after remeasurement of a crystal of Hessenberg, on which he had determined the very complex symbol of the table; *S*: corresponding to a set of angles found even more frequently than those related to *C*. Each of these forms may occur alone on a crystal, along with either of the others or with both. There is nothing to choose between the quality of reflections obtained from all three. Of the other four forms in the table, Irby (2) may be merged with *S*: ; Irby (3), Hessenberg and Cesàro with *C*. Cesàro's symbol was the result of an elaborate calculation of the measurements of a single Lake Superior crystal which chanced to be dominated by the vicinal form *C*. The choice of the particular symbols of *C* and *S*: was in part fixed by the condition that they both lie in the zone determined by *b*: and λ., a rather common rhombohedron. This zone also contains two forms still to be mentioned, 𝔠 and 𝔟.

b: determines with $\{13\bar{4}1\}$ a dominant zone on at least half of the crystals studied. In this zone lie the following forms:

𝔉: $(4.8.\overline{12}.5)$ one of the most common negative scalenohedrons.
F $(5.11.\overline{16}.6)$ Schnorr, 1896. Palache 1898 as new. Established.
A $(6.14.\overline{20}.7)$ Palache, 1898. A weak form seen but twice.
J $(8.20.\overline{28}.9)$ Pirsson, 1891. See below.
I $(7.17.\overline{24}.8)$ Palache, 1898. Now united with J.
Y $(12.32.\overline{44}.13)$ vom Rath, 1877. See below.
B $(12.40.\overline{52}.11)$ Palache, 1898. A weak form but established.

Concerning the forms *J* and *Y* there is much the same story to be told as about *b*:; each is the center of a group of poorly established forms.

			ϕ	ρ	
J	$8.20.\overline{28}.9$	$15.7.\overline{13}$	−13°54′	69°56′	Pirsson, 1891
I	$7.17.\overline{24}.8$	$13.6.\overline{11}$	−13 31½	69 13½	Palache, 1898
	$25.64.\overline{90}.32$	$49.24.\overline{41}$	−14 23½	68 02½	Dana, 1873, no angles
	$9.23.\overline{32}.10$	$17.8.\overline{16}$	−14 10½	70 28½	Gonnard, 1897

The form *J* was found by Pirsson on a crystal supposed to have come from Guanajuato, Mexico. It gave good measurements and was in the zone defined above. Had this form been known to the writer in 1898, the form *I*, which is very near to it, would not have been proposed and is now withdrawn. Gonnard's form from Couzon, France, gave measurements which are almost as close to the angles of Pirsson's form as to the more complex one proposed.

			ϕ	ρ	
Y	$12.32.\overline{44}.13$	$23.11.\overline{21}$	−14°42½′	71°30½′	vom Rath, 1877, New Jersey
	$5.13.\overline{18}.5$	$28.13.\overline{26}$	−14 23½	72 31	Sella, 1856
	$11.29.\overline{40}.12$	$21.10.\overline{19}$	−14 34	71 13½	Levy-vom Rath, 1876, Elba
	$9.24.\overline{33}.10$	$52.25.\overline{47}$	−14 42½	71 04	Franzenau & Vendl, 1930
	$3.8.\overline{11}.3$	$17.8.\overline{16}$	−14 42½	72 50½	Buttgenbach, 1920
	$18.49.\overline{67}.20$	$35.17.\overline{32}$	−14 57½	71 21	vom Rath, 1876: Vendl, 1921

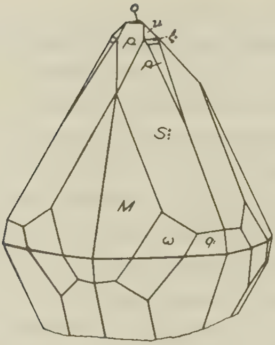

1.

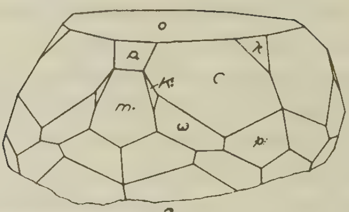

2.

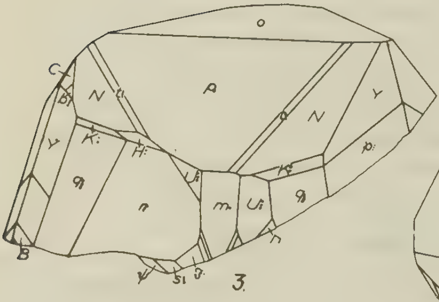

3.

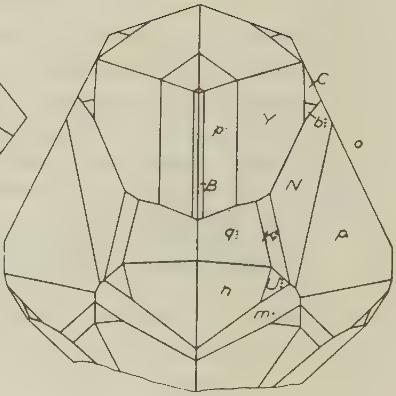

4.

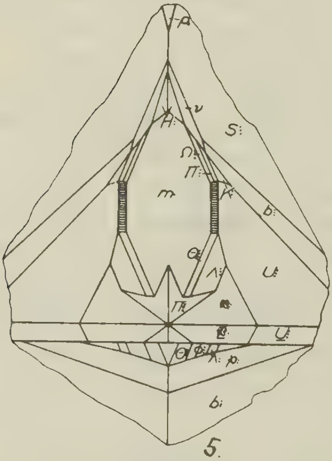

5.

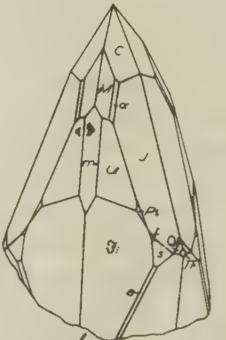

6.

FIG. 1. Calcite showing the forms; *o* $\{0001\}$, *ω* $\{16.16.\overline{32}.9\}$, *p.* $\{10\bar{1}1\}$, *ν.*$\{05\bar{5}4\}$,*ξ.* $\{04\bar{4}3\}$, *ρ.* $\{03\bar{3}2\}$, *M* $\{8.4.\overline{12}.5\}$, 𝔮: $\{24\bar{6}1\}$, *S*: $\{32.56.\overline{88}.45\}$.

FIG. 2. Calcite showing the forms; *o* $\{0001\}$, *ω* $\{16.16.\overline{32}.9\}$, *p.* $\{1011\}$, *m.* $\{40\bar{4}1\}$, λ. $\{08\bar{8}7\}$, *K:* $\{21\bar{3}1\}$, *C* $\{14.26.\overline{40}.21\}$, 𝔭: $\{13\bar{4}1\}$.

These various symbols show that *Y* is in a disturbed region similar to *b*⁝ . The form last listed is maintained by Vendl after extensive discussion of the various alternatives. The measured angles of {9.24.$\overline{33}$.14} are as well satisfied by the angles of *Y*. Buttgenbach's symbol is simpler and rather far removed from *Y* in position, but it is based on poor and widely varying angles. *Y*, on the other hand, was found repeatedly in good position on the author's crystals and by Whitlock at Rondout, New York. It has been observed again on Elba crystals by Grill (1912) who found it a characteristic form for that locality. It seems well justified to regard all these forms as vicinals to *Y*, especially as it alone falls into the important zone under discussion.

I.{17.38.$\overline{55}$.24}, *D*{3.8.$\overline{11}$.4}—These two scalenohedrons form with {01$\bar{1}$2} a zone which very nearly, but not quite, contains *C*. *I*. bears to the strong form {4.8.$\overline{12}$.5} the same relation that *C* bears to *b*⁝ that is of a vicinal to its simpler, stronger form. *D* is also near to *A*, but it is a more definite form and was recognized on ten crystals. *I*. and *D* are shown in Figs. 10 and 11, and their zonal relations are best seen in gnomonic projection (Palache, 1898).

𝔠{4.20.$\overline{24}$.17}, 𝔡{4.36.$\overline{40}$.31}—The first of these forms was reported as new in 1898 but had been recorded from Üto, Sweden, by Sansoni in 1890. The second is met with repeatedly in good position. The two forms lie in the zone determined by *b*⁝ and {08$\bar{8}$7}, already mentioned. They are well shown in Fig. 12 (Palache, 1898).

K{1.11.12.8}—The interest attaching to this form was fully described in the first report. It is a common form but is generally so etched as to be unmeasurable but may be recognized by its sub-cubic shape.

FIG. 3. Calcite, Tamarack Mine, Lake Superior. One half of a twin, drawn in normal position, showing the forms: *o* {0001}, Ψ {10.1.$\overline{11}$.0}, *p*. {10$\bar{1}$1}, *m*. {40$\bar{4}$1}, *K*: {21$\bar{3}$1}, *N* {12.4.$\overline{16}$.11}, *U*⁝ {10.4.$\overline{14}$.3}, 𝔍⁝ {62$\bar{8}$1}, *q*⁝ {9.5.$\overline{14}$.3}, *r*⁝ {32.14.$\overline{46}$.9}, *s*⁝ {16.7.$\overline{23}$.1}, *t*⁝ {37.4.$\overline{41}$.36}, *b*⁝ {35$\bar{8}$4}, *C* {14.26.$\overline{40}$.21}, *Y* {12.32.$\overline{44}$.13}, 𝔭⁝ {13$\bar{4}$1}, *B* {12.40.$\overline{52}$.11}.

FIG. 4. Calcite, Tamarack Mine; same crystal as Fig. 3. Drawn normal to the twin plane, {01$\bar{1}$2} and to a face of the prism {11$\bar{2}$0}. Idealized symmetry of development and smaller faces omitted.

FIG. 5. Calcite, Lake Superior. One coign of a crystal showing the forms: *ν* {11$\bar{2}$1}, *p*. {10$\bar{1}$1}, *m*. {40$\bar{4}$1}, *K*: {21$\bar{3}$1}, *H*: {31$\bar{4}$2}, *U*⁝ {10.4.$\overline{14}$.3}, 𝔓⁝ {51$\bar{6}$1}, Λ⁝ {32.4.$\overline{36}$.7}, Φ⁝ {9.1.$\overline{10}$.2}, Π⁝ {10.1.$\overline{11}$.3}, Θ⁝ {40.4.$\overline{44}$.9}, Ω⁝ {32.2.$\overline{34}$.9}, *b*⁝ {35$\bar{8}$4}, *S*⁝ {32.56.$\overline{88}$.45}. Shows also a basal twin lamella.

FIG. 6. Calcite, Allouez Mine, Lake Superior, showing the forms: *a* {11$\bar{2}$0}, *α* {44$\bar{8}$3}, *m*. {40$\bar{4}$1}, Π. {08$\bar{8}$1}, *P*: {32$\bar{5}$1}, *M* {8.4.$\overline{12}$.5}, *U*⁝ {10.4.$\overline{14}$.3}, 𝔍⁝ {62$\bar{8}$1}, *s* {16.20.$\overline{36}$.5}, *t* {9.13.$\overline{22}$.5}, *C* {14.26.$\overline{40}$.21}, *J* {8.20.$\overline{28}$.9}, *Q*⁝ {7.28.$\overline{35}$.9}. Drawn by Howard T. Evans, Jr.

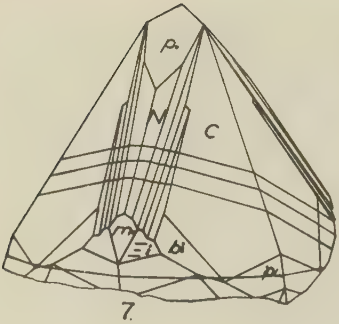

7.

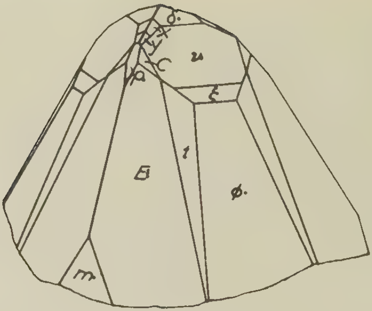

8.

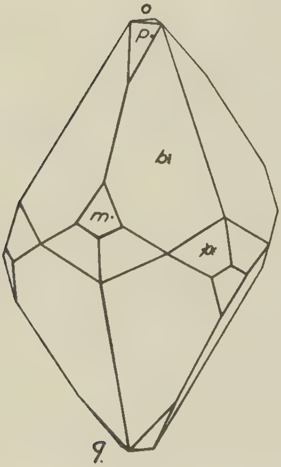

9.

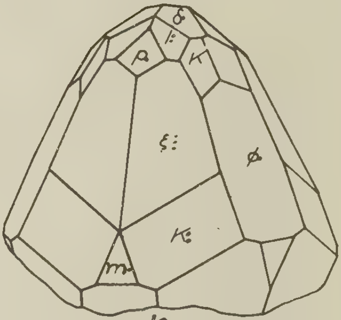

10.

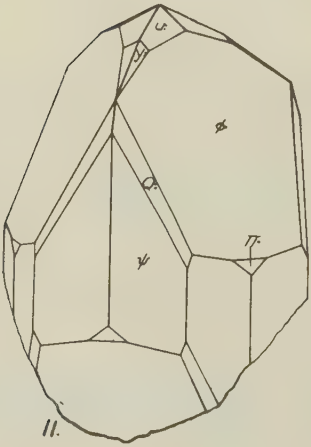

11.

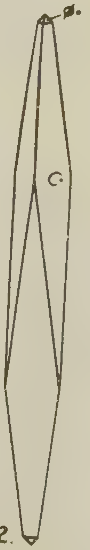

12.

The crystal of Fig. 13 (Palache, 1898) shows it, and it was found with good faces on the crystal shown here as Fig. 10. This form is well established.

Two figures have been added to this paper to show unusual habits for Lake Superior crystals. Figure 11 is remarkable for the large development of the prism $\psi\{10.1.\overline{11}.0\}$, which is found frequently but is generally very subordinate. It was reported as new in 1898 but was found later to have been described elsewhere. Figure 12 shows what is very rare in the whole Lake Superior region, a simple rhombohedral type. However, the form is a rare one $\{0.13.\overline{13}.1\}$.

The paper to which constant reference has been made is "The Crystallization of the Calcite from the Copper Mines of Lake Superior," by Charles Palache, *Geological Survey of Michigan*, Vol. VI, Pt. II—Appendix, pp. 161–184, Plates 11–16, with 24 figures and a gnomonic projection. It will be noticed by any reader who refers to the 1898 paper that the Goldschmidt G_2 and the Naumann crystallographic symbols there used have been discarded. This is in accordance with recent usage in this laboratory. The Bravais symbols used here are given in the older form list along with the others. The letters used for the forms are the same.

The review of the early study has shown the need of the following changes:

A form $P\{13.7.\overline{20}.3\}$ was described on page 176 of that paper and illustrated as a tiny facet in Fig. 7. As this form was not found again, the crystal was remeasured and no measurable face was found at the place indicated. The form is, therefore, withdrawn as based on an inexplicable error.

FIG. 7. Calcite, Lake Superior, showing the forms: *p.* $\{10\bar{1}1\}$, *m.* $\{40\bar{4}1\}$, *N* $\{12.4.\overline{16}.11\}$, Ξ: $\{14.2.\overline{16}.3\}$, *b*: $\{35\bar{8}4\}$, *C* $\{14.26.\overline{40}.21\}$, 𝔭: $\{13\bar{4}1\}$. Twin lamellae parallel to $\{01\bar{1}2\}$ are indicated.

FIG. 8. Calcite, Lake Superior, showing the forms: *p.* $\{10\bar{1}1\}$, *m.* $\{40\bar{4}1\}$, δ. $\{01\bar{1}2\}$, ν. $\{05\bar{5}4\}$, ξ. $\{04\bar{4}3\}$, φ. $\{02\bar{2}1\}$, *y* $\{7.6.\overline{13}.20\}$, *x* $\{4.5.\bar{9}.14\}$, *C* $\{14.26.\overline{40}.21\}$, *E*: $\{5.10.\overline{15}.7\}$, t $\{3.13.\overline{16}.8\}$.

FIG. 9. Calcite, Lake Superior. Illustrating the commonest type of habit in the region. The forms are *o* $\{0001\}$, *p.* $\{10\bar{1}1\}$, *m.* $\{40\bar{4}1\}$, *b*: $\{35\bar{8}4\}$, and 𝔭: $\{13\bar{4}1\}$.

FIG. 10. Calcite from Champion Mine, Lake Superior, showing the forms: *p.* $\{10\bar{1}1\}$, *m.* $\{40\bar{4}1\}$, δ. $\{01\bar{1}2\}$, φ. $\{02\bar{2}1\}$, *l*: $\{32\bar{5}7\}$, *K*: $\{21\bar{3}1\}$, ξ: $\{7.3.\overline{10}.4\}$, and *K* $\{1.11.\overline{12}.8\}$. Drawn by Howard T. Evans, Jr.

FIG. 11. Calcite from Lake Superior. Unusual habit showing as dominant the prism ψ $\{10.1.\overline{11}.0\}$, with φ. $\{02\bar{2}1\}$, Π. $\{08\bar{8}1\}$, *y*: $\{23\bar{5}8\}$, *u*: $\{3.5.\bar{8}.13\}$, and *Q*: $\{19.13.\overline{32}.6\}$.

FIG. 12. Calcite, Lake Superior. Very unusual habit for the region showing chiefly the rhombohedron *C.* $\{0.13.\overline{13}.1\}$, an uncommon form on calcite, with φ. $\{02\bar{2}1\}$.

Figure 11 of the report shows a form letter $\mathfrak{B}$: $\{2.9.\overline{11}.5\}$. This form was by an oversight omitted from the list of forms.

The form $E\{21.35.\overline{56}.44\}$ was listed in the report and shown in Fig. 5, where it truncates the edge between $\{0001\}$ and *b*: $\{35\bar{8}4\}$. It was afterwards found that that part of *b*: which meets the base was actually *S*: and that *E* was in the zone between the base and $\{32.56.\overline{88}.45\}$. To meet this condition the symbol of *E* had to be changed and took the form $\{32.56.\overline{88}.69\}$. This substitution was reported by Whitlock (1910) in his list of calcite forms. The form was not seen again and is regarded as extremely doubtful.

References

Aminoff (1918), Geol. För. Förh., **40,** 273.
Buttgenbach (1920), *Soc. fr. Min., Bull.* **43,** 24.
Cesàro (1891), *Soc. geol. Belg. Ann.*, **18,** 63.
Eakle (1907), *Dept. Geol. Univ. Calif., Bull.* **5,** 91.
Flink (1914), *Ark. Kem. Min.*, **5,** 1.
Franzenau and Vendl (1930), *Mat. Term. tud. Ertes, Budapest,* **47,** 1.
Gonnard (1897), *Soc. fr. Min., Bull.* **20,** 18.
Gordon (1928), *Festschrift V. Goldschmidt,* Pt. 11, 108.
Grill (1912), *Publ. Ist. Studi sup. Firenzi,* Abs. *Zeits. Krist.*, **55,** 387.
Hessenberg (1870), *Senckenb. Natur. Gesell. Abh.*, No. **7.**
Irby (1878), *Inaug. Diss.*, Göttingen.
Palache (1898), *Geol. Surv. Mich.*, **VI,** Pt. II—Appendix, pp. 161–184, Plates 11–16.
Pirsson (1891), *Am. Jour. Sci.*, **41,** 61.
vom Rath (1876), *Pogg. Annal.*, **158,** 414.
Sansoni (1890), *Gior. d. Min.*, **1,** 129.
Schnorr (1896), Abs. *Zeits. Krist.*, **30,** 160.
Sella (1856), *Roy. Acc. Sc. Torino,* II Ser., **17,** 289.
Smith (1927), *Australian Mus. Rec.*, **15,** 313.
Vendl (1921), *Földt. Közl.*, **50,** 131.
Whitlock (1910), *New York State Museum, Mem.* **13.**
——— (1927), *Am. Mus. Nat. Hist., Bull.* **56,** 351.

HEXAGONAL ZONE SYMBOLS AND TRANSFORMATION FORMULAE

C. W. Wolfe,
*Boston University.**

Abstract

Zone symbols in the hexagonal system may be obtained in the usual cross-multiplication manner for three-index symbols by reducing the four-index symbols to three. This is done by adding enough to h, k, and i to reduce one of them to 0. This must be done for both four-index symbols, making the same index 0 in both cases. By dropping this index in both symbols and cross-multiplying, a three-index zone symbol is obtained. This may be changed to a four-index symbol by remembering that h, k, or i is the sum of the other two, multiplied by minus one. The symbol obtained obeys the Weiss zone rule and is the same, regardless of which index was dropped in obtaining the symbol.

Transformation formulae in the hexagonal system are best written as: 1000/0100/0010/000n, where the only change is in the length of the c axis; or as: 1100/0110/1010/000n, where the first and second order prisms are interchanged, and the length of the c axis may or may not be changed.

Mutual orientation of two crystals of different minerals is best described by noting the parallel crystal planes and the parallel crystal edges of the two species. It is a simple matter to determine these in all but the hexagonal system. The determination of zone symbols in the hexagonal system has not been adequately treated in English or French, and the German writings (Niggli, 1926; Weber, 1922)† seem overcomplicated. Hey (1930) has discussed the problem, but because of a faulty premise in his graphic solution his work is somewhat unsatisfactory. The present paper is an attempt to make available in English a simple procedure for obtaining zone symbols in the hexagonal system.

As is well known, the indices of a line, or edge, or zone are really the coordinates of a point translated certain fractions or multiples of unit distances along two or more coordinates from an origin. In all the crystal systems, save the hexagonal, three coordinates are used to indicate the position of any such point and, thus, the position of the line connecting that point with the origin. This designation may refer to a definite direction and a definite position in space or to only a definite direction. Zone symbols are of the latter type.

In the triaxial crystal systems only one symbol is correct for any given zone. In the hexagonal system, however, which is tetra-axial, there is no unique four-index symbol for designating a particular direction of zone. Instead, there are an indefinite number from which, as a matter of convention, one should be chosen.

---

* Contribution from the Department of Mineralogy and Petrography, Harvard University, No. 263.

† This paper was written before the German works were discovered, and since the approach and methods were different, it seemed desirable to proceed with publication.

The heart of the problem lies in an understanding of the relation between symbols based on two and on three horizontal axes. In Fig. 1 it may be seen that the indices which might be ascribed to the point *Z* are limitless. This is further indicated in Table 1. From these it may be seen that any symbol may be changed without altering its essential correctness by simply adding the same number to *h*, *k*, and *i* of the *hkil* symbol. Obviously, there is no limit to the numbers which can be added or subtracted.

TABLE 1. VARIOUS POSSIBLE INDICES OF THE POINT *Z*, FIGS. 1 and 2

$a_1a_2a_3c$	$a_1a_2a_3c$	$a_1a_2a_3c$	$a_1a_2a_3c$
$[\bar{1}\,0\,\bar{3}\,\bar{1}]$	$[0\,1\,\bar{2}\,\bar{1}]$	$[1\,2\,\bar{1}\,\bar{1}]$	$[2\,3\,0\,\bar{1}]$
+1 1 1	1 1 1	1 1 1	1 1 1
$[0\,1\,\bar{2}\,\bar{1}]$	$[1\,2\,\bar{1}\,\bar{1}]$	$[2\,3\,0\,\bar{1}]$	$[3\,4\,1\,\bar{1}]$
+1 1 1	1 1 1	1 1 1	1 1 1
$[1\,2\,\bar{1}\,\bar{1}]$	$[2\,3\,0\,\bar{1}]$	$[3\,4\,1\,\bar{1}]$	$[4\,5\,2\,\bar{1}]$
+1 1 1	1 1 1	1 1 1	1 1 1
$[2\,3\,0\,\bar{1}]$	$[3\,4\,1\,\bar{1}]$	$[4\,5\,2\,\bar{1}]$	$[5\,6\,3\,\bar{1}]$

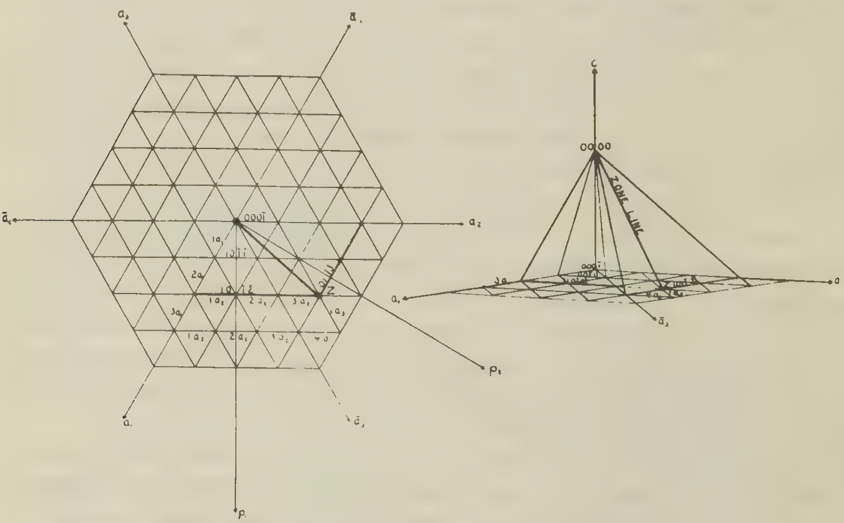

FIG. 1. Hexagonal direct lattice on the plane $c=\bar{1}$, showing the intersection (*Z*) coordinates of the planes (10$\bar{1}$2) and (01$\bar{1}$3).

FIG. 2. Graphic determination of the indices of the edge between (10$\bar{1}$2) and (01$\bar{1}$3). For clarification on the plane $c=\bar{1}$, see Fig. 1 and Table 1.

To reduce the *hkil* symbol to a three-index symbol, it is necessary, however, to make *h*, *k*, or *i* equal to zero, not by simply dropping one of them from the four-index symbol, but by adding a number to each that will result in one of these three indices being zero. This means that there are three unique three-index symbols for every point, depending on which combination of the *a* axes is used. The first step in the determination of a zone symbol is the reduction of the four-index symbol to a three-index symbol as outlined above. Once this has been accomplished the usual cross-multiplication method of obtaining zone symbols is employed. The three-index zone symbol thus obtained is converted to a four-index symbol by the use of the following rule: for the *h*, *k*, and *i* indices, any one of them is the sum of the other two times minus one. The following example will serve to illustrate the procedure.

(1) Determine the three unique three-index symbols for each face (we shall use $(10\bar{1}2)$ and $(01\bar{1}3)$) by adding whatever number is necessary to *h*, *k*, and *i* to reduce each in turn to zero.

$$\begin{array}{lcccccc}
 & a & b & c & a' & b' & c' \\
 & 10\bar{1}2 & 10\bar{1}2 & 10\bar{1}2 & 01\bar{1}3 & 01\bar{1}3 & 01\bar{1}3 \\
 & +111 & 000 & \bar{1}\bar{1}\bar{1} & 111 & \bar{1}\bar{1}\bar{1} & 000 \\
\hline
 & 2102 & 10\bar{1}2 & 0\bar{1}\bar{2}2 & 1203 & \bar{1}0\bar{2}3 & 01\bar{1}3 \\
\text{or} & 21/2 & 1/\bar{1}2 & /\bar{1}\bar{2}2 & 12/3 & \bar{1}/\bar{2}3 & /1\bar{1}3 \\
 & i=0 & k=0 & h=0 & i=0 & k=0 & h=0
\end{array}$$

(2) Cross multiply three-index symbols for which equivalent indices have been dropped.

$$\begin{array}{ll|cccc|l}
 & & & i=0 & & & \\
a & 2 & 1 & 2 & 2 & 1 & 2 \\
a' & 1 & 2 & 3 & 1 & 2 & 3 \\
\hline
 & & \bar{1} & \bar{4} & 3 & & \\
\text{(3) or} & & [\bar{1} & \bar{4} & 5 & 3] &
\end{array}
\qquad
\begin{array}{ll|cccc|l}
 & & & k=0 & & & \\
b & 1 & \bar{1} & 2 & 1 & \bar{1} & 2 \\
b' & \bar{1} & \bar{2} & 3 & \bar{1} & \bar{2} & 3 \\
\hline
 & & 1 & \bar{5} & \bar{3} & & \\
 & & [1 & 4 & \bar{5} & \bar{3}] &
\end{array}
\qquad
\begin{array}{ll|cccc|l}
 & & & h=0 & & & \\
c & \bar{1} & \bar{2} & 2 & \bar{1} & \bar{2} & 2 \\
c' & 1 & \bar{1} & 3 & 1 & \bar{1} & 3 \\
\hline
 & & \bar{4} & 5 & 3 & & \\
 & & [\bar{1} & \bar{4} & 5 & 3] &
\end{array}$$

The last step is shown just above. It is the conversion of the three-index symbol to a four-index one by making the dropped index equal to the sum of the first two of the three-index symbol times minus one.

Figure 2 demonstrates the correctness of the zone symbol $[14\bar{5}\bar{3}]$ as determined above. It may be seen that the coordinates of the point *Z*, which defines the zone symbol, may be $a_1 = \frac{1}{3}$, $a_2 = 4/3$, $a_3 = \bar{5}/3$. This figure should be correlated with Fig. 1 to bring out the relations on the plane where $c = \bar{1}$.

Hey (1930) stated that the four-index zone symbol does not obey the Weiss zone symbol rule.* It will be seen that all of the zone symbols listed in Table 1 plus the one determined above do obey the rule. Taking two of them at random plus the one above we have:

---

* Namely that with a face (*pqrs*) in a zone [*hkil*], the sum of the products $ph + qk + ri + sl = 0$.

$$\begin{array}{ccc} (0\ \ 1\ \ \bar{1}\ \ 3) & (1\ \ 0\ \ \bar{1}\ \ 2) & (1\ \ 0\ \ \bar{1}\ \ 2) \\ \times & \times & \times \\ \underline{[3\ \ 4\ \ 1\ \ \bar{1}]} & \underline{[1\ \ 2\ \ \bar{1}\ \ \bar{1}]} & \underline{[1\ \ 4\ \ \bar{5}\ \ \bar{3}]} \\ 0+4+\bar{1}+\bar{3}=0 & 1+0+1+\bar{2}=0 & 1+0+5+\bar{6}=0 \end{array}$$

Hey's faulty conclusion resulted from an erroneous choice of graphic unit for indexing the intersections on the a_1, a_2, and a_3 axes of the zone line connecting the poles $(10\bar{1}2)$ and $(01\bar{1}3)$. His unit was the distance from the origin to the pole of $(11\bar{2}2)$. The correct graphic unit along the a_1, a_2, and a_3 axes to be used in indexing zone lines is the distance from the center of the projection to the pole of $(11\bar{2}3)$. This is two-thirds of Hey's unit. Figure 3 shows Hey's method of indexing a zone, but the intersection figures given are based on the correct unit. Whereas Hey determined the intersections to be 2, $\frac{1}{2}$ and $\frac{2}{5}$ on a_1, a_2, and a_3 consecutively, the intersections based on the correct unit are 3, $\frac{3}{4}$, and $\bar{3}/5$. Inverting these and making the c intersection equal to $\bar{1}$ we obtain the zone symbol $[14\bar{5}\bar{3}]$ instead of $[14\bar{5}\bar{2}]$ as deduced by Hey.

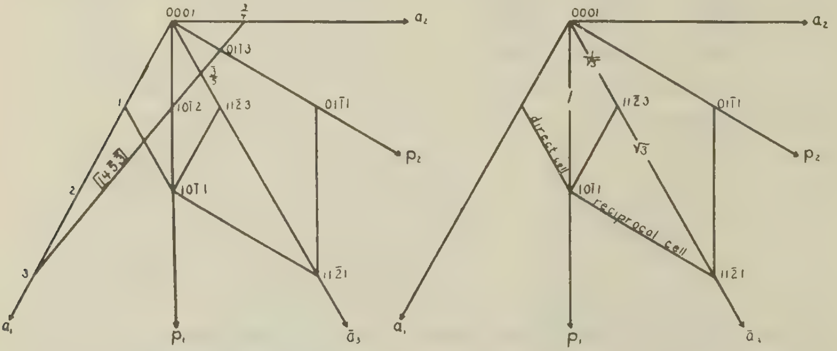

FIG. 3. Gnomonic intercepts on the a axes of the zone line connecting the poles of $(10\bar{1}2)$ and $(01\bar{1}3)$ with unit distance equal to the polar distance of $(11\bar{2}3)$.

FIG. 4. Derivation of the unit length on the a axes for indexing gnomonic zone lines in the hexagonal system.

The choice of $(11\bar{2}3)$ as the unit distance is required by the relation between the reciprocal lattice and the direct lattice in the hexagonal system. Figure 4 shows the reciprocal lattice cell with the face poles which fix it.

If we let the length of the figure's edges be 1, the long diagonal is equal to $\sqrt{3}$. The reciprocal of 1 is 1, and the reciprocal of $\sqrt{3}$ is $1/\sqrt{3}$, which is one third of $\sqrt{3}$. Thus the correct direct lattice unit along the *a* axes is one third the length to $(11\bar{2}1)$ or two thirds that to $(11\bar{2}2)$. This is equivalent to the distance from the projection center to the pole of $(11\bar{2}3)$.

Thus, we see that by calculating according to the above method, or by a graphic determination, the same result is obtained. The *h*/*k* value of this symbol indicates correctly the phi angle of the zone. This symbol, then, of all the possible symbols, is unique and should be used in the designation of zone symbols in the hexagonal system.

TRANSFORMATION FORMULAE

Transformations from the elements of one writer to those of another are usually expressed by means of formulae, the linear type of Barker being commonly used today. In my paper, "Crystallographic Procedures" (1941), I stated in brief the methods for obtaining these formulae but neglected to discuss the special case of the hexagonal system. Two possible choices of axes exist here. The first and second order prisms may be interchanged, and a different unit length for *c* may be used. To obtain a transformation formula in this system, denote the second order prism faces by the symbols (1000), (0100) and (0010), instead of $(2\bar{1}\bar{1}0)$, $(11\bar{2}0)$ and $(\bar{1}2\bar{1}0)$ by a parallel shift to pass through the origin. Next obtain the equivalence of these in the new orientation.

(2) (3)
1000 must equal $10\bar{0}0$ or $10\bar{1}0$
0100 must equal 0100 or $\bar{1}100$
0010 must equal 0010 or $0\bar{1}10$
0001 must equal 000n or 000n

Taking the second and third columns and reading the figures vertically we have the two possible transformation formulae in the hexagonal system:

$$1000/0100/0010/000n$$
or
$$1\bar{1}00/01\bar{1}0/\bar{1}010/000n$$

The second formula indicates an interchange of the first and second order prism positions. These formulae, like those in the triaxial systems, permit the ready determination of face indices in the new position and of the new axial lengths. The same procedure as discussed for the triaxial systems applies here.

ACKNOWLEDGMENTS

Much of the work for this paper was done in the Harvard Mineralogical laboratories, and I wish to express my appreciation for the courtesy extended.

REFERENCES

HEY, MAX H., *Mineral. Mag.*, **22,** 283 (1930).

NIGGLI, PAUL, *Lehrbuch der Mineralogie*, 1, Allgemeine Mineralogie, Zweite Auflage, 117 (1926).

WEBER, LEONHARD, *Zeitz. Krist.*, **57,** 200 (1922–23).

WOLFE, C. W., *Am. Mineral.*, **26,** 55 (1941).

LOW-CHALCOCITE AND HIGH-CHALCOCITE

M. J. BUERGER AND NEWTON W. BUERGER,
Massachusetts Institute of Technology, Cambridge, Mass., and
Postgraduate School, U. S. Naval Academy, Annapolis, Md.

ABSTRACT

Bristol chalcocite has been investigated by the Weissenberg method and by the de Jong-Bouman method. It is orthorhombic, diffraction symbol *mmmAb*— –. The *A*-centered cell has the following dimensions:

$$a = 11.90 \text{ Å}$$
$$b = 27.28$$
$$c = 13.41$$

An *x*-ray diffraction investigation of high-chalcocite has also been made by maintaining a Bristol chalcocite crystal above its inversion temperature of 105° C. This was accomplished by installing a small furnace of special construction within the Weissenberg layer-line screen, with the aid of which the crystal was maintained during the investigation at 112° C. The Weissenberg record shows that high-chalcocite is hexagonal, diffraction symbol 6/*mmmH*6/-*c*-, and has the following cell dimensions:

$$a = 3.89 \text{ Å}$$
$$c = 6.68$$

The low chalcocite cell bears a supercell relation to the high-chalcocite cell; its *a*, *b*, and *c* axes are respectively 3, 4, and 2 times as long as those of the orthohexagonal high-chalcocite cell. The superstructure relationship is to be expected from inversion characteristics.

By utilizing the superstructure relationship of low-chalcocite to high-chalcocite, and the theorem that the symmetry of the superstructure must descend from the symmetry of the basic structure by suppression of repetitions, the space groups of both forms of chalcocite can be determined in spite of the fact that their diffraction symbols permit each of these crystals to have three possible space groups. The results of this reasoning are that the space group of high-chalcocite is $H6mcm$ (D_{6h}^{4}) and the space group of low-chalcocite is $Ab2m$(C_{2v}^{15}).

INTRODUCTION

Until recently the opinion has prevailed that low-chalcocite was orthorhombic and that on heating it inverted at 91°C. to an isometric form.[1] A study[2] of the system Cu_2S–CuS has revealed, however, that this is partially true, partially untrue. Low-chalcocite of pure Cu_2S composition indeed inverts on heating; the transformation occurs at 105°C. but the high form is not isometric. On the other hand, chalcocite somewhat lower in copper than ideal Cu_2S breaks up on heating into high-chalcocite and an isometric crystalline phase, digenite.[3] The composition of digenite has a considerable range, centering about Cu_9S_5.

---

[1] Posnjak, Eugene, Allen, E. T., and Merwin, H. E., The sulphides of copper: *Econ. Geol.*, **10,** 491–535 (1915).

[2] Buerger, Newton W., The chalcocite problem: *Econ. Geol.*, **36,** 19–44 (1941).

[3] Buerger, Newton W., *X*-ray evidence for the existence of the mineral digenite, Cu_9S_5: *Am. Mineral.*, **27,** 712–716 (1942).

Evidently digenite is the same as what has been called "isometric chalcocite,"[4] but the symmetry of true high-chalcocite is still unknown. The only structural characteristics of low-chalcocite which are known are the cell dimensions, and there is disagreement about these. It is the chief function of this paper to report an investigation which supplies the symmetries and cells of both low-chalcocite and high-chalcocite and to point out certain relationships which exist between them. The entire investigation was carried out using untwinned fragments of crystals from the Bristol, Connecticut, chalcocite. Copper x-radiation was employed throughout.

LOW-CHALCOCITE

The cell characteristics of low-chalcocite were first investigated by Alsen[5] using the powder, Laue, and rotation methods. The Laue photographs confirmed the accepted orthorhombic symmetry. Layer line spacing data from rotation photographs for the three crystallographic axes indicated the following cell:

	ratio
$a=11.8$ Å	.434
$b=27.2$	1
$c=22.7$	.834

In connection with a more extended study of copper and silver sulfides, selenides, and tellurides, Rahlfs[6] reinvestigated low-chalcocite using the rotation and oscillation methods. He obtained the following cell values:

$a=11.8$ Å
$b=26.9$
$c=13.4$

Rahlfs observed that his value for c differed from Alsen's value, and called attention to Alsen's difficulty in adjusting the crystal for the c axis rotation. He explained Alsen's high value as probably having been caused by rotating the crystal about [102] instead of about the c axis.

We have investigated low-chalcocite both by the equi-inclination Weissenberg method and by the equal-cone de Jong-Bouman method. The Weissenberg films include photographs of the zero, 1st, 2nd, and 3rd levels for the c axis rotation; zero and 2nd levels for the a axis rotation; and zero and 2nd levels for the b axis rotation. The de Jong films include the zero, 1st, 2nd, 3rd, 4th, 5th, and 6th levels for the *c* axis rotation. Simple rotating crystal photographs were also made for rotations about each of the three crystallographic axes.

---

[4] Schneiderhöhn, Hans, and Ramdohr, Paul, *Lehrbuch der Erzmikroskopie* II, 289 (Gebrüder Borntraeger, Berlin, **1931**).

[5] Alsen, Nils, Ueber die Kristallstrukturen von Covellin (CuS) und Kupferglanz (Cu_2S): *Geol. För. I Stockholm Förh.*, **53**, 117–118 (1931).

[6] Rahlfs, Paul, Ueber die kubischen Hochtemperaturmodifikationen der Sulfide, Selenide und Telluride des Silbers und des einwertigen Kupfers: *Zeits. phys. Chem.* (B), **31**, especially p. 193 (1936).

The zero level *c* axis photographs are plainly pseudohexagonal, Fig. 1. The hexagonaloid character is dimensionally very close.

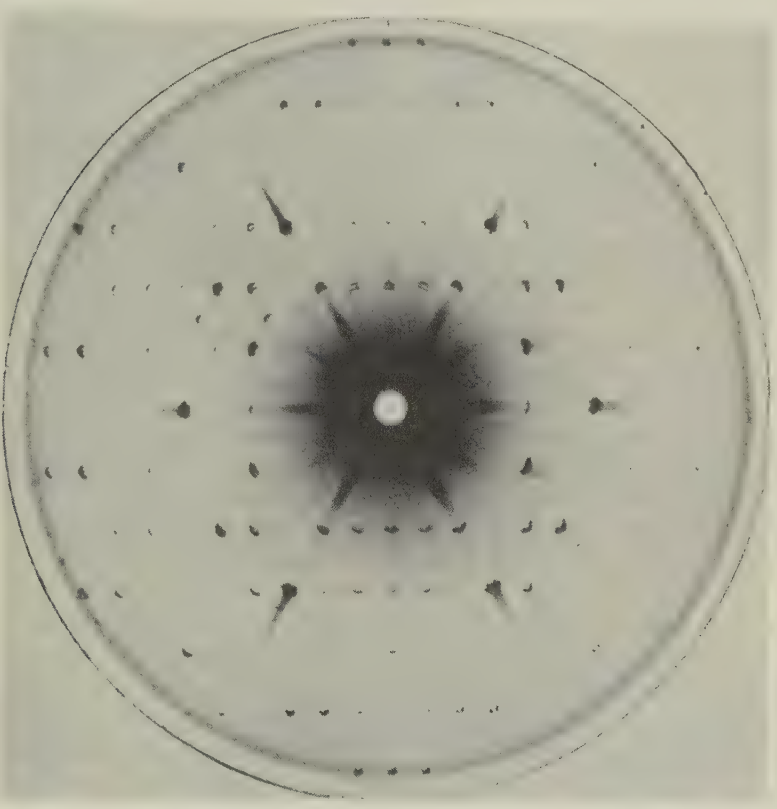

FIG. 1. de Jong-Bouman photograph, low-chalcocite, *c* axis rotation, zero level, $\mu = 45°$, Cu Kα radiation filtered through nickel foil. Note pseudo-hexagonal distribution of strongest spots, and overall symmetry C_{2l}. (A few spots without symmetrically related companions are due to a tiny satellitic twin fragment on one side of the main crystal.)

The level photographs plainly show the crystal to have diffraction symmetry *mmm*. The diffraction symbol *mmmAb*— — is required by the missing reciprocal lattice points. This permits the space group of low-chalcocite to be either *Abmm*, *Ab2m*, or *Abm2*. (The last two are different orientations of the same space group, C_{2v}^{15}, both of which are consistent with the diffraction data.) It will be shown later that the correct space group is probably *Ab2m*.

The cell dimensions of low-chalcocite are (accuracy, about 1%):

	ratio
$a=11.90$ Å	.437
$b=27.28$	1
$c=13.41$	.492

For a density[1] of 5.8 g./c.c., these dimensions call for 96 Cu_2S per cell.

It will be noted that our cell dimensions are in substantial agreement with Rahlf's.

HIGH-CHALCOCITE

In order to investigate the symmetry and cell of high-chalcocite, a furnace was devised[7] for maintaining the crystal at an elevated temperature in a Weissenberg apparatus. This heating unit is similar to that used in the controlled-temperature powder camera,[8] but is so arranged that it is contained within the layer-line screen of the Weissenberg apparatus. For investigating chalcocite, the crystal was maintained at 112°C. (i.e., above the inversion temperature, 105°C.).

An untwinned fragment of Bristol chalcocite was first summarily investigated at room temperature by means of a *c* axis rotation photograph and a *c* axis zero-layer Weissenberg photograph. The temperature of the crystal was then raised to 112°C., and the following photographs were taken for *c* axis rotations while the crystal was maintained at this temperature: simple rotation photograph and equi-inclination Weissenberg resolutions of the zero, 1st, 2nd, and 3rd layers.

The relation between the *c* axis photographs taken for the crystal held at room temperature and at 112°C. is shown in Fig. 2. When the crystal is heated through the inversion, the rotation photographs show that the *c* axis translation becomes halved and the Weissenberg photographs show that the symmetry changes from pseudohexagonal orthorhombic to true hexagonal. This is accompanied by a reduction in the other cell dimensions and consequent vanishing of many of the spots on the zero-level Weissenberg photographs, Fig. 3.

The crystal was also investigated, while being maintained at 112°C., with the aid of rotation photographs and zero and 2nd level equi-inclination Weissenberg photographs for rotations about the *a* axis and about the $[\bar{1}10]$ axis (i.e., the orthohexagonal *b* axis).

---

[7] Buerger, Newton W., Weissenberg controlled-temperature technique. *Program and Abstracts*, Twenty-second Annual Meeting, Mineralogical Society of America, December 29–31 (**1941**) pages [8]-[9].

[8] Buerger, M. J., Buerger, Newton W., and Chesley, Frank G., Apparatus for making *x*-ray powder photographs at controlled, elevated temperatures: *Am. Mineral.*, **28,** 285–302 (1943).

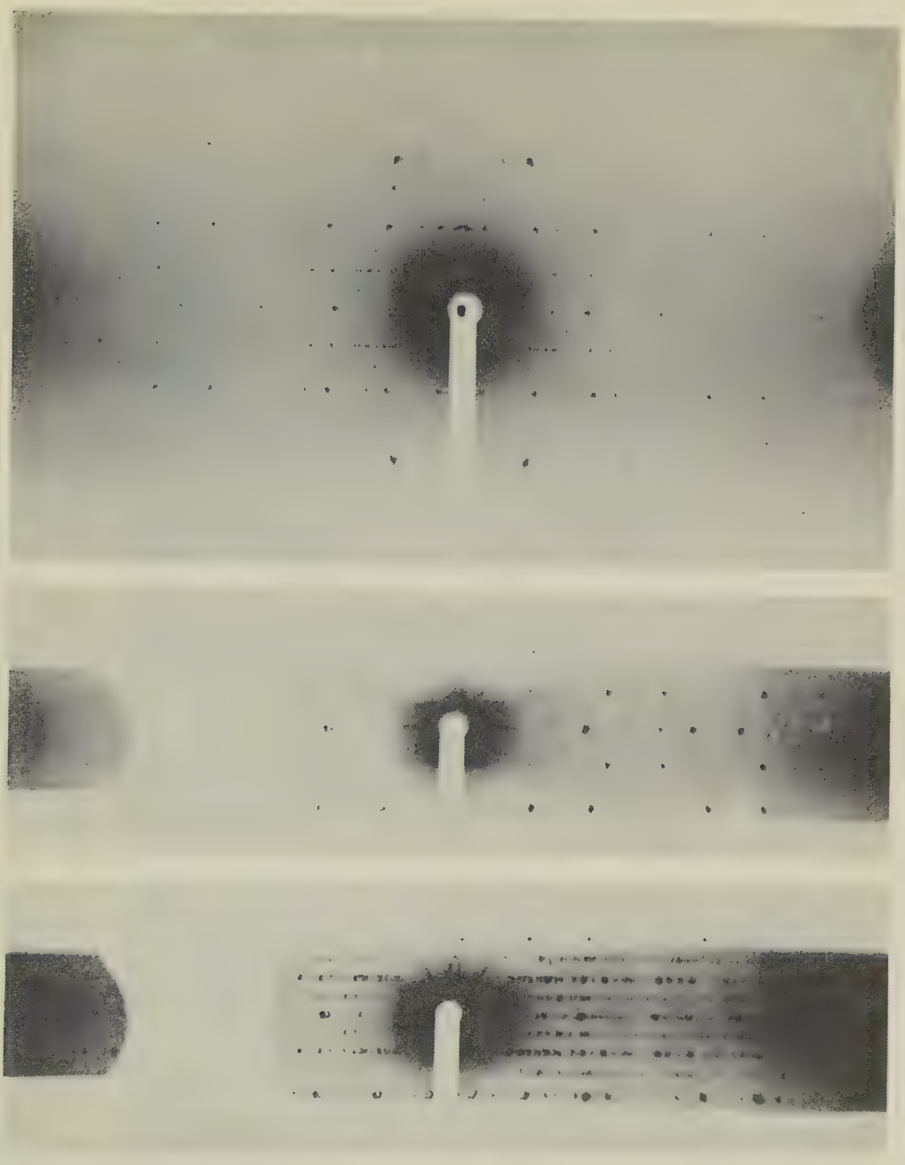

FIG. 2. Rotating-crystal photographs of chalcocite for *c* axis rotation, Cu Kα radiation filtered through nickel foil.

Upper photograph: low-chalcocite crystal.

Middle photograph: high-chalcocite crystal resulting from heating low-chalcocite crystal to 112° C.

Lower photograph: low-chalcocite resulting from cooling the high-chalcocite crystal of the middle photograph to room temperature.

Note that the layer line spacing in the middle photograph is about twice that of the upper photograph, indicating a *c* translation of about half that for the upper photograph. Note, also, that (making allowances for differences in apparatus which affect recording range and *x*-ray beam divergence) the upper and lower photographs are substantially the same, indicating that the transformation from low- to high-chalcocite is reversible.

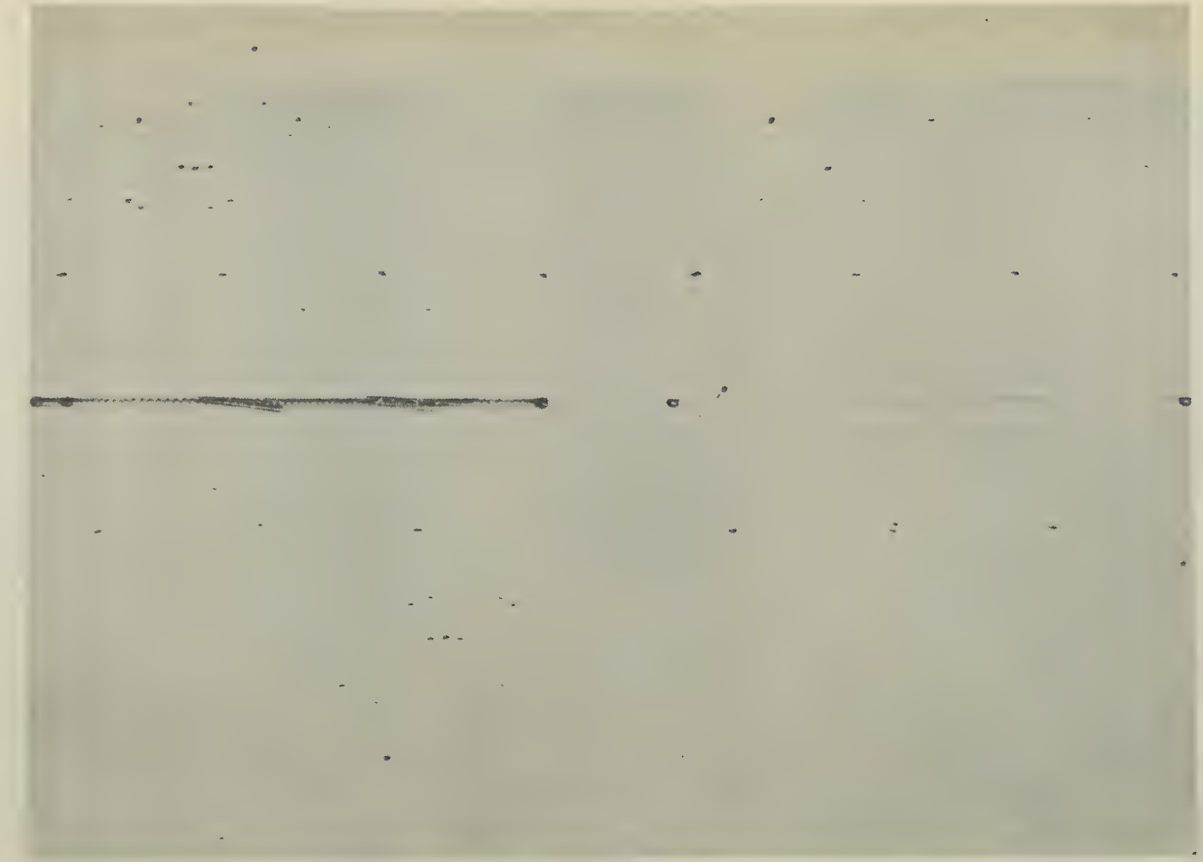

FIG. 3. Weissenberg photographs of chalcocite, *c* axis, zero layer, Cu Kα radiation filtered through nickel foil.
Left photograph: original low-chalcocite crystal.
Right photograph: high-chalcocite crystal resulting from heating low-chalcocite crystal to 112° C.
Note that the left photograph has all the spots of the right photograph plus some additional ones due to the superstructure.
(A few weak spots are due to a satellitic fragment on the main crystal.)

The Weissenberg photographs of high-chalcocite reveal that its diffraction symmetry is $6/mmm$. Missing reciprocal lattice points require the diffraction symbol $6/mmmH-/-c-$. This permits the space group of high-chalcocite to be either $H6/mcm$, $H6cm$, or $H\bar{6}c2$. It will be shown subsequently that the correct space group is probably $H6/mcm$.

The unit cell of high-chalcocite has the following dimensions (accuracy, about 1%):

	ratio
$a = 3.89$Å	1
$c = 6.68$	1.717

According to Sahmen and Tammann,[9] the specific volumes of chalcocite above and below the inversion do not differ by more than .00012 c.c./gm.; so that no appreciable error is made in taking the density of high-chalcocite as 5.8 g./c.c. For this density, the hexagonal cell contains $2Cu_2S$.

RELATIONSHIPS BETWEEN HIGH-CHALCOCITE AND LOW-CHALCOCITE

Dimensional Relationships.—It is known[1,2] that low-chalcocite and high-chalcocite are connected by a rapid transformation. This calls for small structural displacements at the inversion and consequently it is not surprising that, as has been briefly indicated in the last section, the lattice periods of the two forms of chalcocite are related in a simple fashion. The relationship is graphically illustrated in Fig. 4.

The dimensional relationships between the two forms of chalcocite can be represented in several ways. Indicating properties of the high form by the subscript H and of the low form by the subscript L, and using vector notation, the lengths and directions of the cell edges of the two forms of chalcocite are very approximately related as follows:

$$\begin{aligned} \mathbf{a}_L &= 3\mathbf{a}_{1H} + 3\mathbf{a}_{2H} \\ \mathbf{b}_L &= -4\mathbf{a}_{1H} + 4\mathbf{a}_{2H} \\ \mathbf{c}_L &= \qquad\qquad\quad 2\mathbf{c}_H \end{aligned}$$

This can be compactly represented by the matrix of these equations:

Low-chalcocite (doubly primitive, A-centered)
from
High-chalcocite (primitive hexagonal)

$$\left\| \begin{matrix} 3 & 3 & 0 \\ \bar{4} & 4 & 0 \\ 0 & 0 & 2 \end{matrix} \right\|, \text{ modulus } 48.$$

---

[9] Sahmen, R. v., and Tammann, G., Über das Auffinden von Umwandlungspunkten mit einem selbsregistrierenden Dilatographen: *Ann. der Phys.* (4), **10**, 881 (1903).

The 48-fold multiplicity of the low-chalcocite supercell is somewhat misleading because for convenience the orthorhombic prismatic lattice is described by an *A*-centered, and consequently, doubly-primitive, cell.

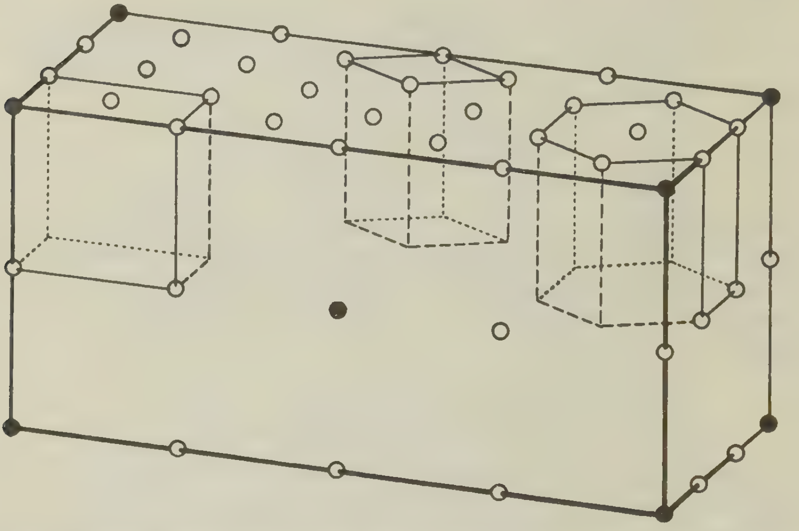

FIG. 4. Relation between the low-chalcocite cell and various cells chosen from the high-chalcocite lattice. The black dots are the lattice points of low-chalcocite, and the large block represents its *A*-centered cell. The open dots are lattice points of high-chalcocite. Three kinds of high-chalcocite cells are outlined; from left to right these are: orthohexagonal unit cell, primitive hexagonal unit cell, and hexagon cell.

The multiplicity of the primitive orthorhombic low-chalcocite supercell is only 24.

The relationship between the cells of the two forms of chalcocite can perhaps better be appreciated by referring the hexagonal, high-chalcocite cell to orthohexagonal axes. The cells of the two forms then compare as follows:

	Low-chalcocite, *A*-centered, orthorhombic cell	*High-chalcocite,* orthohexagonal cell
	$a=11.90$ Å	3.89 Å ($\times 3=11.67$ Å)
	$b=27.28$	6.79 ($\times 4=27.16$ Å)
	$c=13.49$	6.68 ($\times 2=13.36$ Å)
cell contents	96 Cu_2S	4 Cu_2S ($\times 24=96$ Cu_2S)

Thus, the transformation from high-chalcocite to low-chalcocite is accompanied by multiplication of the lengths of the identity periods in the three orthogonal directions, such that the a axis is tripled, the b axis is quadrupled, and the c axis is doubled. This relationship can be compactly represented by the matrix:

Low-chalcocite (doubly primitive, A-centered)
from
High-chalcocite (doubly primitive, orthohexagonal)

$$\begin{Vmatrix} 3 & 0 & 0 \\ 0 & 4 & 0 \\ 0 & 0 & 2 \end{Vmatrix}, \text{ modulus } 24.$$

Symmetry Relationships.—Valuable information can be obtained by comparing the distribution of symmetry in the two chalcocite modifications. Since the orthohexagonal high-chalcocite cell is oriented parallel to the orthorhombic low-chalcocite cell, the symmetry symbols of the high-chalcocite will be written, for purposes of this comparison, in the sequence standard for orthorhombic crystals.

The diffraction symbols and the possible space groups they may indicate, for low- and high-chalcocite, are shown in the following tabulation:

	High-Chalcocite	Low-Chalcocite
Diffraction Symbol	$mmmC-c-$	$mmmAb--$
Included Space Groups	$Cmcm$	$Abmm$
	$Cmc6$	$Ab2m$
	$C2c\bar{6}$	$Abm2$

Now, it was demonstrated in the last section that a supercell dimensional relation exists between the two forms of chalcocite. It is extremely likely that superstructural symmetry relations also exist between them. The most fundamental theorem governing the symmetry of a superstructure is that it must be derivable from the symmetry of the basic structure by suppression of certain elementary repetitions.[10] This requires that one or more of the space groups possible for low-chalcocite must be derivatives of one or more of the space groups possible for high-chalcocite. The above table indicates that, so far as x-ray data are concerned, three possible low-chalcocite space groups are possible derivatives of three possible high-chalcocite space groups, giving nine possible derivations.

Whether a derivation is possible or not can be conveniently studied by utilizing the complete Mauguin space group symbols[11] instead of the usual international abbreviated symbols. In the accompanying table, the complete Mauguin symbol of the high-chalcocite space group is placed above the complete Mauguin symbol for the low-chalcocite space group for each of the nine possible derivations. The arrow indicates the direction of the derivation. In this tabulation, an x is placed below an indicated derivation which is impossible.[11]

---

[10] This will be discussed in greater detail elsewhere.

[11] Buerger, M. J., *X-ray Crystallography*, table 7, pages 84–89, second column.

Note that only one possible derivation of low-chalcocite symmetry from high-chalcocite symmetry is entirely without x's, indicating that this entire low-chalcocite symmetry can be derived from the high-chalcocite symmetry. It is difficult to avoid the conclusion that these two space groups are the correct ones for low-chalcocite and high-chalcocite, respectively.

Transforming these symbols to abbreviated international form, and to normal sequence in the hexagonal case, the space groups for these crystals are as follows:

High-chalcocite	$H6/mcm$	(D_{6h}^4)
Low-chalcocite	$Ab2m$	(C_{2v}^{16})

If this analysis is correct, it is important to note that one of its consequences is that the crystal class of low-chalcocite is not holohedral, but hemimorphic (pyramidal) $m2m$.

$$\begin{array}{llccc} & C & \frac{2}{m} & \frac{2}{c} & \frac{6_3}{m} \\ \downarrow & A & \frac{2}{b} & \frac{2}{m} & \frac{2}{m} \\ & & & x & x \end{array} \qquad \begin{array}{llccc} & C & m & c & 6_3 \\ \downarrow & A & \frac{2}{b} & \frac{2}{m} & \frac{2}{m} \\ & & x & x & x \end{array} \qquad \begin{array}{llccc} & C & 2 & c & \bar{6} \\ \downarrow & A & \frac{2}{b} & \frac{2}{m} & \frac{2}{m} \\ & & x & x & x \end{array}$$

$$\begin{array}{llccc} & C & \frac{2}{m} & \frac{2}{c} & \frac{6_3}{m} \\ \downarrow & A & b & 2 & \mathrm{m} \end{array} \qquad \begin{array}{llccc} & C & m & c & 6_3 \\ \downarrow & A & b & 2 & m \\ & & & x & x \end{array} \qquad \begin{array}{llccc} & C & 2 & c & \bar{6} \\ \downarrow & A & b & 2 & m \\ & & x & x & x \end{array}$$

$$\begin{array}{llccc} & C & \frac{2}{m} & \frac{2}{c} & \frac{6_3}{m} \\ \downarrow & A & b & m & 2 \\ & & & x & x \end{array} \qquad \begin{array}{llccc} & C & m & c & 6_3 \\ \downarrow & A & b & m & 2 \\ & & & x & x \end{array} \qquad \begin{array}{llccc} & C & 2 & c & \bar{6} \\ \downarrow & A & b & m & 2 \\ & & x & x & x \end{array}$$

CONCLUSION

This paper should not be concluded without pointing out how correctly Groth[12] had critically appraised the relationship between low- and high-chalcocite. He contended that a transformation from orthorhombic low-chalcocite to the supposed isometric high-chalcocite ought to involve important volume changes, which Sahmen and Tammann[9] had not found in the region of the transformation. From this Groth concluded that the resistance changes which occurred when heating orthorhombic chalcocite through the region near 100°C. and noted by Hittorff[13] and Mönch[14] were related to some other kind of transition, not to a transformation from orthorhombic chalcocite to "isometric chalcocite." We now know that this view was correct; that orthorhombic chalcocite does not invert to "isometric chalcocite" (i.e., digenite). As Groth surmised, there is a somewhat different relation occurring at the true chalcocite transition, namely, the two structures are very similar, the transition involving no great volume changes, but merely a slight shifting of the atomic arrangement such that the low-form assumes a superstructure based upon the basic structure of the high-form.

---

[12] Groth, P., *Chemische Kristallographie*, **1**, 135 (1906).

[13] Hittorff, Ueber das electrische Leitungsvermögen des Schwefelsilbers und Halbschwefelkupfers: *Ann. Phys. u. Chem.*, **84**, 1–28 (1851).

[14] Mönch, Willy, Ueber die elektrische Leitfäigkeit von Kupfersulfür, Silber-, Blei-, und schwartzem Quecksilbersulfid: *Neues Jahrb. Min.*, etc., B. B. **20**, 365–435 (1905).

NOTES AND NEWS

THE SYSTEM $Fe_2O_3-Mn_2O_3$: SOME COMMENTS ON THE NAMES BIXBYITE, SITAPARITE, AND PARTRIDGEITE

Brian Mason

Early in 1942 I published a paper (1) in which I pointed out the structural identity and chemical similarity of bixbyite and sitaparite (both can be represented by the formula $(Mn,Fe)_2O_3$), and suggested that the name sitaparite be discarded in favor of bixbyite, which has priority. My attitude is summed up in a sentence from that paper: " . . . the mineral name bixbyite may be defined precisely as including all specimens with manganese, iron, and oxygen as principal components, and having the same crystal lattice as the original bixbyite from Utah." On the basis of this definition the name bixbyite would include all specimens from pure Mn_2O_3 up to the limiting substitution of iron in place of manganese. Recently, however, de Villiers (2, 3) has disagreed with this scheme, and instead proposes to retain the name sitaparite, and in addition describes as a new species—partridgeite—natural Mn_2O_3 with only small replacement of manganese by iron. In his words: ". . . I suggest that the name partridgeite be applied to those manganese-iron sesquioxides containing less than 10% Fe_2O_3, sitaparite to the sesquioxides containing between 10% and 30% Fe_2O_3, and bixbyite to the mineral with more than 30% Fe_2O_3."

As Fleischer says in a commentary to de Villier's proposals (3), arguments can be advanced for both of the above views, and the interpretation preferred is chiefly a matter of convenience. From that point of view there is little reason to carry the discussion further. However, in order to obtain a more precise knowledge of the mutual relations of these minerals I spent some time in 1942 in working out the phase diagram for the Fe_2O_3-Mn_2O_3 system. This work and the discussion of the mineralogical aspects was recently published in full in the *Geologiska Föreningens i Stockholm Förhandlingar* (4). As, however, this publication is not at present available outside Europe, a summary of the results may be given here, as the phase diagram provides the only satisfactory basis for the discussion of the mineralogical aspects of this system.

The phase diagram (Fig. 1) was built up by the use of synthetic preparations covering systematically all compositions between Fe_2O_3 and Mn_2O_3 at intervals of 10 mol.% and occasionally also at 5 mol.%. These preparations were heated in air at different temperatures between 600° and 1000° until equilibrium was reached, and the phase composition of the products determined by means of powder photographs.

In the present discussion it is unnecessary to consider the Fe_2O side of the phase diagram. The feature which concerns us is the replacement in the Mn_2O_3 structure of manganese by iron. The diagram shows that the maximum replacement of manganese by iron is nearly 30% at 600°

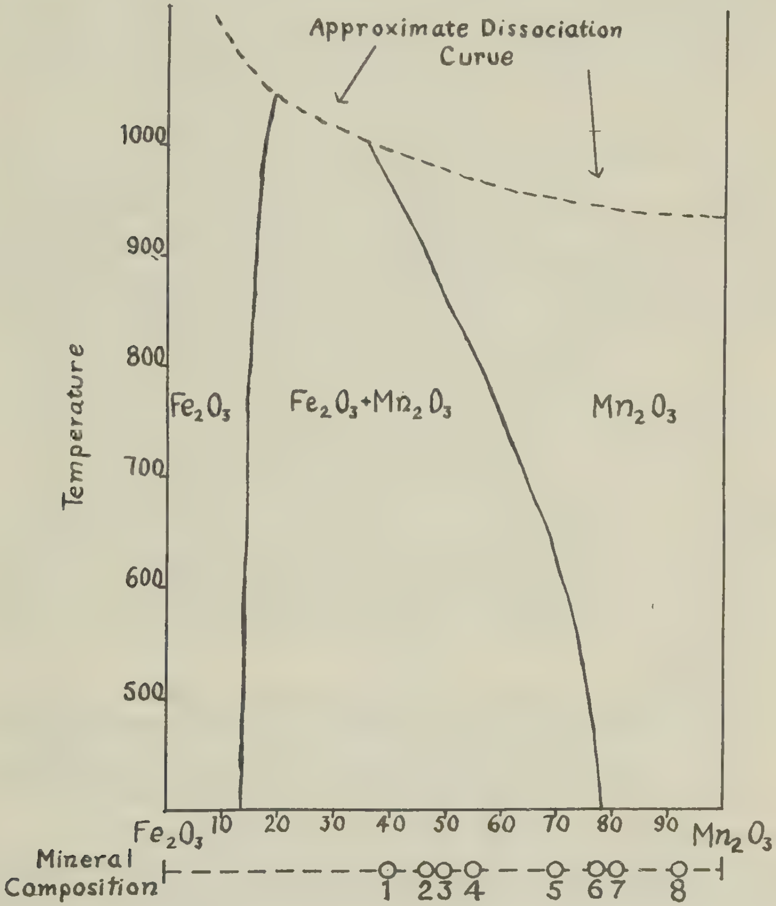

FIG. 1. The system Fe_2O_3-Mn_2O_3. Mineral localities: 1 and 2, Rio Chubut, Patagonia; 3, Thomas Range, Utah; 4, Black Range, New Mexico; 5, Sitapar, India; 6, Långban, Sweden; 7 and 8, Postmasburg, South Africa.

and increases rapidly with temperature, reaching somewhat over 60% at 1000°. At temperatures greater than 1000° the sesquioxides dissociate.

The chemical composition of recorded minerals of this group are also plotted in Fig. 1. According to my proposals all these should be referred to the one species, bixbyite. According to de Villiers specimens 1–4 are bixbyite, specimens 5, 6, and 7 are sitaparite, and specimen 8 is partridgeite.

On a paragenetic basis it is possible to arrange these specimens in two groups, the one group—specimens 1–4—being those of fumarolic or pneumatolytic origin, the other group—specimens 5–8—being of metamorphic origin. The specimens of the first group are all associated with acid extrusives, generally rhyolites, and occur together with such minerals as quartz, feldspar, topaz, and hematite (specularite). The specimens of the second group all come from metamorphosed manganese ores.

The noteworthy feature is that these two groups do not overlap in composition. The specimens of fumarolic or pneumatolytic origin group in the interval 45–60% Fe_2O_3, those of metamorphic origin between 0–30% Fe_2O_3. The explanation is contained in the phase diagram. Specimens containing more than 45% Fe_2O_3 can only be formed at temperatures of about 800° or higher, whereas specimens with 0–30% Fe_2O_3 can be formed at temperatures of about 650° and less.

It is evidently unlikely that specimens of $(Mn,Fe)_2O_3$ with more than 30% Fe_2O_3 will be found in metamorphosed ores, unless the temperature of metamorphism has been unusually high. Thus the composition range of the specimens of metamorphic origin is not likely to overlap that of the specimens of pneumatolytic and fumarolic origin. It is evident that the latter have been formed at temperatures of about 800°–1000°, and the almost constant association of hematite with them shows that they were formed in a medium rich in Fe_2O_3. Thus they probably contain the maximum amount of Fe_2O_3 possible at the temperature and pressure of formation.[1]

This discussion reveals that the homogeneous mineral $(Mn,Fe)_2O_3$ can be subdivided into two groups, falling into two composition ranges:

1. Those of pneumatolytic or fumarolic origin, with Fe_2O_3 content from 40–60%.
2. Those occurring in metamorphosed manganese ores, with Fe_2O_3 content from 0–30%.

It might appear that I have made a good case for the division of the $(Mn,Fe)_2O_3$ group of minerals into two species—bixbyite for all specimens of pneumatolytic origin, the original bixbyite having been of this type, and sitaparite for all specimens of metamorphic origin, the original sitaparite having been of this type. However, I still do not think that such a subdivision is necessary. Mode of origin is no principle on which to base mineralogical systematics, any more than age is a basis for petrological systematics. The specific name bixbyite, as I defined it above, covers the $(Mn,Fe)_2O_3$ group satisfactorily. However, if it is desired to subdivide the group, then subdivide rationally, into bixbyite and sitaparite. The introduction of the name partridgeite is an unnecessary complication, serving no useful purpose.

---

[1] From the phase diagram it can be seen that specimens of $(Mn,Fe)_2O_3$ of fumarolic and pneumatolytic origin should be in a metastable state at normal temperatures, tending to disintegrate into an intergrowth of a hematite phase and a $(Mn,Fe)_2O_3$ phase with a much lower content of Fe_2O_3. Specimens from Utah which I have examined show, however, no trace of any such disintegration. Evidently the rate of cooling was too great for readjustment.

References

1. Mason, B., Bixbyite from Långban. The identity of bixbyite and sitaparite: *Geol. Fören. Förh.*, **64**, 117–125 (1942).
2. de Villiers, J. E., A preliminary description of the new mineral partridgeite: *Am. Mineral.*, **28**, 336–338 (1943).
3. de Villiers, J. E., and Fleischer, M., A discussion: Bixbyite-sitaparite-partridgeite: *Am. Mineral.*, **28**, 468–469 (1943).
4. Mason, B., Mineralogical aspects of the system FeO-Fe_2O_3-MnO-Mn_2O_3: *Geol. Fören. Förh.*, **65**, 97–180 (1943).

BOOK REVIEWS

MINERALS AND ROCKS, THEIR NATURE, OCCURRENCE AND USES, BY RUSSELL D. GEORGE. The Century Earth Science Series. Pp. 595, Pl. 48, Figs. 141. D. Appleton-Century Co. **1943**. Price $6.00.

At first glance one is staggered by the encyclopedic scope of this volume, which runs to 568 pages, exclusive of glossary and index. A list of the main headings will show the ground covered:

Part I

Metallic Elements and Minerals

Chapter I	Materials of the earth and properties of minerals	9 pages
Chapter II	Metalliferous ore deposits	14 pages
Chapter III	Iron, steel and alloy metals	46 pages
Chapter IV	Major non-ferrous industrial metals	43 pages
Chapter V	Minor metals of increasing industrial value	20 pages
Chapter VI	Precious and semi-precious metals	15 pages
Chapter VII	Alkali metals	16 pages
Chapter VIII	Semi-metals	15 pages
Chapter IX	The radioactive series	13 pages
Chapter X	Minor metals of limited industrial value	8 pages

Part II

Nonmetallic Elements and Minerals

Chapter XI	Carbon and hydrocarbon minerals and rocks	35 pages
Chapter XII	Sulphur, phosphorus and the halogens	8 pages
Chapter XIII	Water and the atmosphere	8 pages
Chapter XIV	Gem minerals and semi-precious stones	11 pages

Part III

Rock-making minerals

Chapter XV	Important primary minerals	21 pages
Chapter XVI	Minor and secondary minerals	18 pages
Chapter XVII	Industrial uses of rock-making minerals	10 pages

Part IV

Determinative mineralogy

Chapter XVIII	Equipment and tests	4 pages
Chapter XIX	Identification of elements and minerals	26 pages
Chapter XX	Igneous rocks: general	15 pages
Chapter XXI	Igneous rock families	36 pages
Chapter XXII	Sedimentary rocks	22 pages
Clapter XXIII	Metamorphic rocks	8 pages
Chapter XXIV	Industrial uses of rocks	24 pages

Appendix: Materials classified by uses

It will obviously be impracticable to review in detail this mass of material, but the more important points may be touched upon. In general, the author and the publisher are to be complimented on the almost complete absence of typographical and subject matter errors. The outstanding fault is the entire lack of references to original sources, a lack which limits the value of the work for all but the most elementary purposes. It is true that such references, which might well have been grouped at the end of each chapter, would have expanded the already voluminous text, but some of the minor points could have been eliminated, and the added value of references would have more than compensated for any loss of material. Another unfortunate feature is in the drawings of crystals, many of which are made with curious orientations. Moreover, the appearance of the drawings is seriously impaired by poor draughtsmanship, resulting in uneven heaviness of lines, and unnecessary distortion of crystal faces, which mars the appearance of the whole production. The figures on pages 14, 17, and 19 are particular offenders in this respect, but faulty drawing and orientation persist throughout the text. This is the only obvious flaw in an otherwise excellently produced publication. There are numerous photographic reproductions illustrating mineral and rock types and occurrences, which form an excellent feature of the work.

The general physical properties of minerals are covered briefly but adequately. In the chapter on ore deposits the author outlines the occurrence of different types of deposits, illustrating with idealized diagrams, which might better have been taken from specific deposits, as was done for a few cases.

The ferrous metals and alloy metals, such as chromium, molybdenum, tungsten, etc., are dealt with first from the metallurgical standpoint, following which is a condensed mineralogical description of the compounds in which they occur. In these descriptions the composition of limonite is given without remark as if it were a single definite mineral rather than a group. Rare minerals, like pharmacosiderite, are described in unnecessary detail, and this emphasis on rare minerals is consistently applied throughout the book. On page 76 it is noted as "possible" that nickel occurs in pyrrhotite as grains of pentlandite, whereas in most occurrences this has been clearly demonstrated to be true.

The non-ferrous industrial metals are listed as including Cu, Pb, Zn, Cd, Sn, Al, Mg, Hg. Again, as with iron, many rare varieties are described, although there is an additional list merely mentioned by name.

There is an interesting chapter on minor metals which are of increasing economic value, such as Be, Ca, Sr, Ba, the radium group, and Nb, Ta, Ti, Zr, giving lists of their uses. In the chapter on precious metals, gold, silver and the platinum group are covered briefly.

The uses, sources, and mineralogic descriptions of the alkali metals, Li, Na, K, Rb, Cs, are given, even including the descriptions of many uncommon minerals. Under the semimetals are treated As, Sb, Bi, Se, Te. The discussion of the radioactive series is more chemical than mineralogical, as is that of the group of rare elements in Chapter X which do not in general form distinctive minerals. These elements include gallium, indium, scandium, hafnium, etc., and the rare earths.

Under the non-metallic elements considerable space is devoted to carbon in the form of coal and peat, and petroleum, with a discussion of their origin, production, by-products and uses. Graphite and diamond receive brief mention. The chapter on sulphur, phosphorus, and the halogens is short, giving the chemical properties and uses of the elements, and descriptions of the definite minerals, when such occur. The chapter on atmospheric gases and water might very well have been omitted entirely. Under gem minerals is given the mineralogic descriptions of the principal precious and semi-precious stones, listing under each the names and properties of the sub-varieties, a very convenient arrangement in comparison with a purely alphabetical classification.

The rock-forming minerals are divided into the primary minerals, first of the igneous, then of the sedimentary rocks. Minor primary minerals, such as sphene, zircon, etc., are treated in the section with the secondary minerals. These should more fittingly have been included as an appendix to the primary group. The secondary minerals are grouped as zeolites; minerals of weathering (such as the clays, etc.); minerals of metamorphism (not in general duplicating those also common in igneous or sedimentary rocks). No effort has been made to group stress and non-stress minerals. There is a separate chapter on the industrial uses of rock-forming minerals—quartz, mica, feldspars, clays, refractories, etc., to some extent duplicated in the section on the industrial uses of rocks.

Part IV lists and describes apparatus and reagents for simple determinative tests with blowpipe and chemicals, but does not attempt to give determinative tables, except one brief color and luster classification. There is the usual description of flame and bead colors, plaster tablet reactions, and an alphabetical list of the elements with tests for most of them.

The final section is the petrology of the common rocks, starting with a general outline of the formation of igneous rocks, their textures and occurrence, and a field classification modified from Cross, Iddings, Pirsson, Washington. Each group of the classification is then taken up in some detail with respect to its mineralogy. For the sedimentary rocks there is a good, brief statement of the conditions of weathering of older rocks, and transportation of the resulting materials. This is followed by the normal descriptive classification into subgroups, ending with chemical precipitates. Under metamorphic rocks, the metamorphic processes are outlined, in simple brief form; then follows a classification and description of types (as foliates or non-foliates, because of the occasional difficulty of determining the character of the parent rock).

In the chapter on industrial uses of rocks, building stones are treated at considerable length, covering strength, durability (with a rather detailed discussion of the causes of decomposition, especially in buildings), workability, color, etc. Cements, limes, plaster and clays are treated somewhat less fully.

An appendix, in which materials (mineral or elements) are grouped by uses, should be useful in some cases.

It seems that the author has tried to take in too much territory in too much detail, and the result has been an unwieldy volume, which on this account will be less useful than it might have been. Admittedly, setting the limit on volume and detail is a difficult problem, and Mr. George has done perhaps as well as possible with the ground he has covered. He has served a useful purpose at least in assembling under one cover a very considerable and varied supply of information.

JOSEPH MURDOCH

OPTICAL CRYSTALLOGRAPHY, BY ERNEST E. WAHLSTROM. v+206 pages. John Wiley and Sons, New York, **1943**. Price $3.00.

This little volume will be a welcome addition to the many books in this field. Its contribution lies almost wholly in the multitude of excellent two- and three-dimensional drawings which are by far the best the reviewer has seen.

As a textbook it has many weaknesses. The presentation of ray velocity surfaces, the Fresnel ellipsoid, the ovaloid, and Bertin's surface will unnecessarily confuse the student who finds it difficult enough to grasp the essential fundamentals without going so far afield. Twenty-nine of the two hundred and six pages are devoted to the determination of the optic sign, an incidental feature of the optical properties of a crystal, and the determination of the principal indices of refraction are correspondingly neglected. The method for the determination of the principal indices of refraction of a uniaxial crystal (page 87) applies only to crystals of low double refraction and is not applicable to most organic compounds which are characterized by high double refraction.

There are numerous errors such as the statement on page 79, "The quartz wedge resolves white light into its spectrum." The equations of the various optical surfaces are given in rectangular coordinates but on pages 65 and 142 the equations do not follow the text. Although perhaps not of major significance, these errors will confuse the student. However, the reviewer still believes that the experienced teacher can use this book to advantage because of the many excellent drawings it contains.

C. B. Slawson

NEW MINERAL NAMES

Hectorite

H. Strese and U. Hofmann: Synthesis of magnesium silicate gels with two-dimensional regular structure. *Zeit. anorganische allgemeine Chemie*, **247**, 65–95 (1941).

The name hectorite is proposed for the magnesian bentonite from Hector, California, described by W. F. Foshag and A. O. Woodford, *Am. Mineral.*, **21**, 238–244 (1936). It is regarded as being the magnesium end-member of the montmorillonite group. *X*-ray data are given.

Discussion: The name hectorite was proposed in 1882 for an alteration product of pyroxene, perhaps anthophyllite (see *Dana's System*, 6th Ed., p. 364). However, the name has not been used in this sense for many years.

Michael Fleischer

Brammallite

F. A. Bannister: Brammallite (sodium-illite), a new mineral from Llandebie, South Wales. *Mineral. Mag.*, **26**, 304–307 (1943).

Name: For Dr. Alfred Brammall.

Chemical Properties: A member of the illite group of mica-like clay minerals, which contains more Na than K.

Analysis by M. H. Hey on 15 mg. gave Na_2O 5.22, K_2O 2.58%. (i.e. the full alkali content of paragonite. M. F.)

No measurable differences were found in the *x*-ray patterns of material heated to 700°.

Physical Properties: Occurs as white, compact tufts of elongated plates about $\frac{1}{2}$ mm. long. Optically biaxial, negative, $\alpha = 1.561 \pm .002$, $\gamma = 1.579 \pm .002$, 2 V large. The extinction is nearly parallel. Elongation positive. *X*-ray study gave $a = 5.2$, $b = 9.0$, $c \sin \beta = 18.95$ Å. *X*-ray powder data are given.

Occurrence: Occurs as fissure filling and surface coating on shale overlying coal-measures at Llandebie, South Wales.

M. F.

REDEFINITION OF SPECIES

Jacobsite, Vredenburgite

Brian Mason: Mineralogical aspects of the system FeO-Fe_2O_3-MnO-Mn_2O_3. *Geol. För. Förh.* (Stockholm), **65**, 97–180 (1943).

In a study of the system Fe_3O_4-Mn_3O_4, natural material in the range 54–91% Mn_3O_4 was found to consist of two phases: a tetragonal phase with 91% Mn_3O_4 and a cubic phase with 54% Mn_3O_4. It is suggested that the name vredenburgite should be used for all compositions within this range. These consist of oriented intergrowths formed by ex-solution.

It is possible that material might be found in this range in which ex-solution did not occur. If such homogeneous tetragonal material is found, it is suggested that it be termed β-vredenburgite.

Jacobsite is usually considered to be $MnFe_2O_4$. It is suggested that the name be extended to include those members of the cubic solid solutions of the series Fe_3O_4-Mn_3O_4 in which the theoretical $MnFe_2O_4$ molecule is dominant, i.e. $(Fe,Mn)_3O_4$ containing 16.7–54% Mn_3O_4. Some MgO is commonly present.

M. F.

DISCREDITED MINERALS

Devadite, Garividite

BRIAN MASON, *Op. Cit.* Devadite and garividite were names suggested by Fermor (1938) for material differing slightly in Fe_3O_4-Mn_3O_4 ratio from vredenburgite. If the definition of vredenburgite is extended as stated above, these names become superfluous and should be discarded.

M. F.

Mr. George L. English, Manager of the Mineral Department of Ward's Natural Science Establishment from 1913 to 1922 and consulting mineralogist from 1922 until his retirement in 1934, died January 2, 1944, at Winter Park, Florida, at the age of 79 years. Mr. English served as Vice-president of the Mineralogical Society of America in 1927.